Temonen et al., 1996). Thus, to understand its pathogenesis, it is important to discern host immune responses to the virus, particularly hantavirus-specific $CD8^+$ cytotoxic T lymphocytes (CTLs). The interaction of hantavirus-specific CTLs with the hantavirus remains unclear. In contrast to humans, the reservoir animals are persistently infected without signs of disease (Meyer and Schmaljohn, 2000).

In a previous study, we established a persistent infection model by inoculating mice with a sublethal dose of Hantaan virus (HTNV), the prototype of the genus *Hantavirus*, within 24 h of birth. The number of interferon (IFN)-γ-inducible HTNV-specific $CD8^+$ T cells first increased in the acute phase and then decreased to an undetectable level soon thereafter. Viral antigen was detected in the lung until 90 days after the infection, although no HTNV-specific $CD8^+$ T cells were observed at that time; T cells reappeared at 120 days, although no detectable viral antigen was present in the lung (Araki et al., 2003). A similar suppression and reappearance of HTNV-specific $CD8^+$ T cells was observed using a severe combined immune deficiency (SCID) mouse model in which spleen cells from immunocompetent BALB/c mice were passively transferred to SCID mice 14 days after infection (Araki et al., 2004a). These results indicated that disseminated HTNV infection before the induction of an immune response is important for the establishment of persistent infection and the suppression of HTNV-specific $CD8^+$ T cells in mice. HTNV-specific $CD8^+$ T cells were induced in HTNV-infected nude mice after adoptive transfer of spleen cells from immunocompetent BALB/c mice (Araki et al., 2004a), indicating that the HTNV-specific $CD8^+$ T cells appearing in SCID or nude mice were produced by the transferred cells. This suggests that the peripheral $CD8^+$ T cell response is more important than the thymus in suppressing specific T cell responses in persistently infected mice.

Although several N-specific CTL epitopes have been determined in C57BL/6 mice, as yet, none has been reported in BALB/c mice (Park et al., 2000; Maeda et al., 2004, 2005). To further analyze the $CD8^+$ T cell response, we first identified the immunodominant CTL epitope in the HTNV nucleocapsid protein (N), an abundant antigen of hantaviruses, in BALB/c mice. We then established an epitope-specific MHC tetramer assay and sequentially analyzed the epitope-specific $CD8^+$ T cell response by comparing the transient infection model and the persistent infection model.

Results

Screening for the N-specific $CD8^+$ T cell epitope in BALB/c mice

We used HTNV-infected P388D1 cells (H-2^d) as antigen-presenting cells to detect all antigen-specific $CD8^+$ T cells. Accordingly, we used BALB/c mice (H-2^d) for screening. In total, 105 15-mer peptides with 10 amino acid overlaps, encompassing the entire HTNV N protein, were divided into seven pools (Table 1). The peptide mixtures from each pool were screened for their capacity to stimulate IFN-γ production in spleen cells from BALB/c mice infected with HTNV. Based on the FACS analysis, the peptide mixture from pool 6 was able to induce IFN-γ (Fig. 1A). Approximately 20% of all antigen-specific $CD8^+$ T cells were raised as N-specific cells (Fig. 1A). Next, we examined the peptides in pool 6 (nos. 81–94) individually, and determined that peptides 83 and 84 were positive for IFN-γ induction (Fig. 1B). To identify the minimum sequence of the T cell epitope, we examined seven additional 11-mer peptides, encompassing the sequence represented in peptides 83 and 84. As shown in Fig. 1C, peptides 108 and 109 stimulated HTNV-specific $CD8^+$ T cells, while peptides 106, 107, and 110 did not. Because a 9-mer peptide is recommended for synthesis of MHC class I tetramers, we examined the shorter sequence ILQDMRNTI (N335–343), which was suggested from the results with peptides 108 and 109. As shown in Fig. 1D, this peptide induced IFN-γ (0.14%), and we thus deemed it the sole epitope for N-specific $CD8^+$ T cells in BALB/c mice (H-2^d).

Determination of MHC restriction in sequence NP335–343

To determine the MHC restriction of the HTNV-specific response to this peptide derived from N, an inhibition-of-peptide-stimulation assay was conducted using antibodies specific to the class I molecules D^d or K^d. The percentage of peptide-specific $CD8^+$ T cells was 0.04% with the anti-H-$2D^d$ antibody and 0.01% with the anti-H-$2K^d$ antibody (Fig. 2). Although the percentage of positive cells was lower than measured in the same experiment in Fig. 1, the peptide stimulation was only blocked by the antibody to H-$2K^d$, indicating that the epitope was H-$2K^d$-restricted. The percentage of positive cells varied depending on the condition of the cells. We obtained reproducible results from several independent experiments; therefore, we deemed this to be of significance. In addition, we also confirmed H-$2K^d$ binding affinity using the Bioinformatics and Molecular Analysis Section (BIMAS) algorithms (available at http://thr.cit.nih.gov/molbio/hla_bind/) (Parker et al., 1994). The sequence of the N335–343 peptide scored the highest in H-$2K^d$ (69.12), but lowest in H-$2D^d$ (0.54) and H-$2L^d$ (1.5). The specific motif for peptides that bind H-$2K^d$ is believed to be a nonamer, with tyrosine or phenylalanine residues in the second amino acid position, and leucine or isoleucine in the carboxyl-terminal or ninth amino acid position as dominant anchoring positions. Although the sequence that we identified does not have an aromatic residue in the second position, it is similar to that of the HIV-1 gag epitope (AMQMLKETI), which also does not contain an anchoring aromatic residue in position two (Mata et al., 1998). These results also suggest that the N335–343 peptide is H-$2K^d$-restricted. Thus, a tetramer was prepared that consisted of H-$2K^d$ molecules loaded with the N335–343 peptide; it was named NP335–343.

Response of NP335–343-specific $CD8^+$ T cells in a transient infection model

To evaluate the effect of NP335–343 staining on epitope-specific $CD8^+$ T cells, we first stained spleen cells from the transient infection mouse model. The frequency of NP335–343-positive cells, as a percentage of total $CD44^+$ $CD8^+$ T

Table 1
Peptide library derived from the full-length N protein: overlapping peptides used to test IFN-γ-inducing ability

Peptide	AA position	Sequence	Peptide	AA position	Sequence	Peptide	AA position	Sequence	Peptide	AA position	Sequence
Pool 1			Pool 2			Pool 3			Pool 4		
1	1–15	MMATMEELQREINAH	17	65–79	QLADRIATGKNLGKE	33	129–143	SFVVPILLKALYMLT	49	193–207	EITPGRYRTAVCGLY
2	5–19	MEELQREINAHEGQL	18	69–83	RIATGKNLGKEQDPT	34	133–147	PILLKALYMLTTRGR	50	197–211	GRYRTAVCGLYPAQI
3	9–23	QREINAHEGQLVIAR	19	73–87	GKNLGKEQDPTGVEP	35	137–151	KALYMLTTRGRQTTK	51	201–215	TAVCGLYPAQIKARQ
4	13–27	NAHEGQLVIARQKVR	20	77–91	GKEQDPTGVEPGDHL	36	141–155	MLTTRGRQTTKDNKG	52	205–219	GLYPAQIKARQMISP
5	17–31	GQLVIARQKVRDAEK	21	81–95	DPTGVEPGDHLKERS	37	145–159	RGRQTTKDNKGTRIR	53	209–223	AQIKARQMISPVMSV
6	21–35	IARQKVRDAEKQYEK	22	85–99	VEPGDHLKERSMLSY	38	149–163	TTKDNKGTRIRFKDD	54	213–227	ARQMISPVMSVIGFL
7	25–39	KVRDAEKQYEKDPDE	23	89–103	DHLKERSMLSYGNVL	39	153–167	NKGTRIRFKDDSSFE	55	217–231	ISPVMSVIGFLALAK
8	29–43	AEKQYEKDPDELNKR	24	93–107	ERSMLSYGNVLDLNH	40	157–171	RIRFKDDSSFEDVNG	56	221–235	MSVIGFLALAKDWSD
9	33–47	YEKDPDELNKRTLTD	25	97–111	LSYGNVLDLNHLDID	41	161–175	KDDSSFEDVNGIRKP	57	225–239	GFLALAKDWSDRIEQ
10	37–51	PDELNKRTLTDREGV	26	101–115	NVLDLNHLDIDEPTG	42	165–179	SFEDVNGIRKPKHLY	58	229–243	LAKDWSDRIEQWLIE
11	41–55	NKRTLTDREGVAVSI	27	105–119	LNHLDIDEPTGQTAD	43	169–183	VNGIRKPKHLYVSLP	59	233–247	WSDRIEQWLIEPCKL
12	45–59	LTDREGVAVSIQAKI	28	109–123	DIDEPTGQTADWLSI	44	173–187	RKPKHLYVSLPNAQS	60	237–251	IEQWLIEPCKLLPDT
13	49–63	EGVAVSIQAKIDELK	29	113–127	PTGQTADWLSIIVYL	45	177–191	HLYVSLPNAQSSMKA	61	241–255	LIEPCKLLPDTAAVS
14	53–67	VSIQAKIDELKRQLA	30	117–131	TADWLSIIVYLTSFV	46	181–195	SLPNAQSSMKAEEIT	62	245–259	CKLLPDTAAVSLLGG
15	57–71	AKIDELKRQLADRIA	31	121–135	LSIIVYLTSFVVPIL	47	185–199	AQSSMKAEEITPGRY	63	249–263	PDTAAVSLLGGPATN
16	61–75	ELKRQLADRIATGKN	32	125–139	VYLTSFVVPILLKAL	48	189–203	MKAEEITPGRYRTAV	64	253–267	AVSLLGGPATNRDYL
Pool 5			Pool 6			Pool 7					
65	257–271	LGGPATNRDYLRQRQ	81	321–335	LFIAGIAELGAFFSI	95	377–391	LGQRIIVLFMVAWGK			
66	261–275	ATNRDYLRQRQVALG	82	325–339	GIAELGAFFSILQDM	96	381–395	IIVLFMVAWGKEAVD			
67	265–279	DYLRQRQVALGNMET	83	329–343	LGAFFSILQDMRNTI	97	385–399	FMVAWGKEAVDNFHL			
68	269–283	QRQVALGNMETKESK	84	333–347	FSILQDMRNTIMASK	98	389–403	WGKEAVDNFHLGDDM			
69	273–287	ALGNMETKESKAIRQ	85	337–351	QDMRNTIMASKTVGT	99	393–407	AVDNFHLGDDMDPEL			
70	277–291	METKESKAIRQHAEA	86	341–355	NTIMASKTVGTSEEK	100	397–411	FHLGDDMDPELRTLA			
71	281–295	ESKAIRQHAEAAGCS	87	345–359	ASKTVGTSEEKLRKK	101	401–415	DDMDPELRTLAQSLI			
72	285–299	IRQHAEAAGCSMIED	88	349–363	VGTSEEKLRKKSSFY	102	405–419	PELRTLAQSLIDVKV			
73	289–303	AEAAGCSMIEDIESP	89	353–367	EEKLRKKSSFYQSYL	103	409–423	TLAQSLIDVKVKEIS			
74	293–307	GCSMIEDIESPSSIW	90	357–371	RKKSSFYQSYLRRTQ	104	413–427	SLIDVKVKEISNQEP			
75	297–311	IEDIESPSSIWVFAG	91	361–375	SFYQSYLRRTQSMGI	105	416–430	DVKVKEISNQEPLKL			
76	301–315	ESPSSIWVFAGAPDR	92	365–379	SYLRRTQSMGIQLGQ						
77	305–319	SIWVFAGAPDRCPPT	93	369–383	RTQSMGIQLGQRIIV						
78	309–323	FAGAPDRCPPTCLFI	94	373–387	MGIQLGQRIIVLFMV						
79	313–327	PDRCPPTCLFIAGIA									
80	317–331	PPTCLFIAGIAELGA									

The amino acid position indicates the location of the indicated sequences in the N protein.

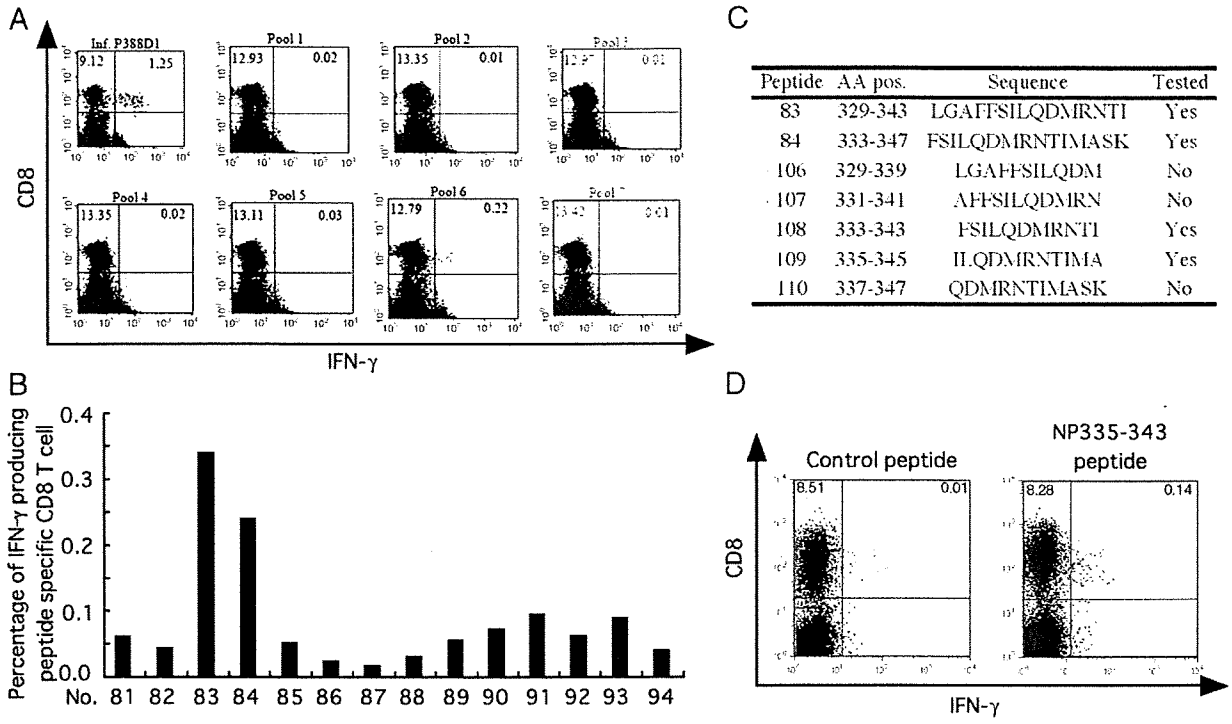

Fig. 1. Peptide screening for the N protein epitope from infected adult mice. Spleen cells were obtained from HTNV-infected BALB/c mice 10 days after HTNV inoculation. Spleen cells were cultured in the presence of brefeldin A and IL-2. IFN-γ^+ $CD8^+$ cells were detected using flow cytometry. The numbers are the percentages of IFN-γ^+ $CD8^+$ cells. (A) Spleen cells were cultured with HTNV-infected P388D1 cells (positive control) or with peptide pools (Table 1). IFN-γ positive cells were detected only with pool 6 peptides. (B) Spleen cells were cultured with peptides 81–94 from pool 6. IFN-γ-positive cells were detected using peptides 83 and 84. (C) Spleen cells were cultured with or without peptides 106–110 derived from peptides 83 and 84. IFN-γ-positive cells were detected using peptides 108 and 109. (D) Spleen cells were cultured with peptide 93 (negative control) or NP335–343 derived from peptides 110 and 112. The NP335–343 peptide stimulated $CD8^+$ cells to produce IFN-γ.

cells, increased 7 days after infection, with a peak at 10 days after infection (1.11%); it then decreased at 3 weeks after infection and continued at a low level thereafter (Figs. 3A, B). The same kinetic profile was produced by NP335–343 peptide-specific, IFN-γ-inducible $CD8^+$ T cells 3, 7, 12, and 14 days post infection (data not shown). Furthermore, these kinetics were similar to those of virus-specific, IFN-γ-inducible $CD8^+$ T cells (Fig. 3C). NP335–343-specific $CD8^+$ T cells comprised approximately 20% of all antigen-specific $CD8^+$ T cells (Figs. 3B, C). This is in good correspondence to previous data (Fig. 1A). These data indicated that the transient infection model had a normal immune response and that the tetramer NP335–343 could detect epitope-specific $CD8^+$ T cells.

Response of NP335–343-specific $CD8^+$ T cells in a persistent infection model

Next, we examined the kinetics involved in NP335–343 staining of epitope-specific $CD44^+$ $CD8^+$ T cells in a persistent infection mouse model. As a result, a very low level of NP335–343-specific $CD8^+$ T cell response was observed at all time points. NP335–343-specific $CD8^+$ T cells tended to appear just before viral antigen elimination (13 weeks after infection [0.31%]; Fig. 4A). The total number of NP335–343-positive $CD44^+$ $CD8^+$ T cells was equal to or lower than the lowest level in the transient infection model (Figs. 3C and 4C). The same tendency was seen in the NP335–343 peptide stimulation assays performed at 2, 5, 8, 10, 13, and 17 weeks (data not shown).

In our previous study with this model, we found that the IFN-γ-producing $CD8^+$ T cell response appeared in the acute phase, and was then quickly suppressed in the following viral persistent phase. IFN-γ-producing $CD8^+$ T cells reappeared at about 17 weeks after infection, when the persistent infection ended (Araki et al., 2003). We examined the kinetics of the IFN-γ-producing $CD8^+$ T cells in more detail and confirmed that the IFN-γ-producing cell response was very weak compared to that in the transient infection model. It appeared twice, at 2 weeks after infection and just before viral antigen elimination (Fig. 4C). We found suppression of IFN-γ-production and also suppression of NP335–343-specific $CD8^+$ T cell production. We looked for, but did not detect, other N-specific $CD8^+$ T cell epitopes in this model (data not shown). These results indicate that hantavirus strongly suppresses the production of N-specific $CD8^+$ T cells in the persistent infection model (Fig. 5).

Discussion

We identified an N-specific $CD8^+$ T cell epitope in BALB/c mice ($H\text{-}2^d$). Specifically, we found one major epitope in BALB/c mice corresponding to amino acids 335–343 of the HTNV N protein, which was $H\text{-}2K^d$-restricted. At least three epitopes have been found within HTNV N in C57BL/6 mice (H-

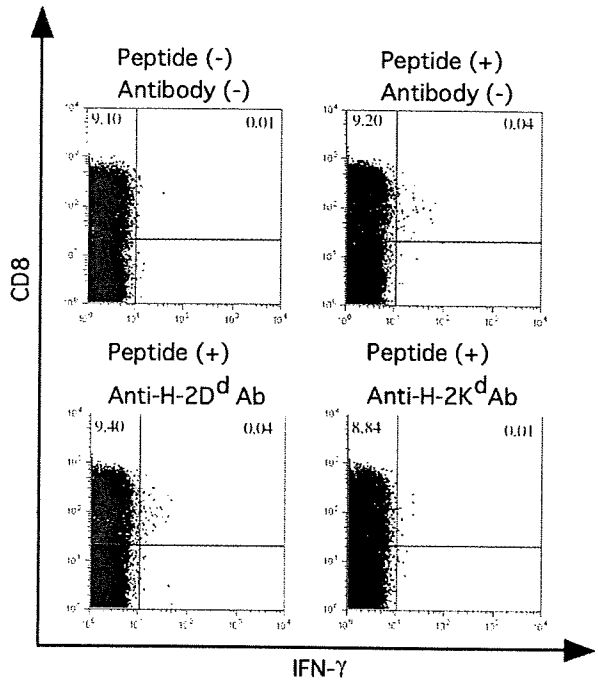

Fig. 2. The NP335–343 peptide is MHC class I H-2K^d-restricted. Spleen cells were obtained from HTNV-infected BALB/c mice 10 days after HTNV inoculation. Spleen cells were cultured in the presence of brefeldin A and IL-2. When required, anti-H-2D^d or H-2K^d antibodies were added simultaneously with or without the NP335–343 peptide. IFN-γ$^+$ CD8$^+$ cells were detected using flow cytometry. The numbers are the percentages of IFN-γ$^+$ CD8$^+$ cells.

2^b) by the BIMAS prediction algorithm (Park et al., 2000). The previously identified epitopes NP3 (amino acids 221–228: SVIGFLAL), NP4 (amino acids 328–335: LGAFFSIL), and NP7 (amino acids 422–429: SNQEPLKL) were different from our identified epitope, but NP4 does partially overlap with it. For Sin Nombre virus (SNV) infection, peptide screening in B6. PL Thy1^a/Cy mice (H-2^b) identified four epitopes, NC94–101 (SSLRYGNV), NC175–189 (minimal epitope:SMPTAQSTM), NC211–225, 217–231 (minimal epitope:SPVMGVIGF or PVMGVIGFS), and NC331–345 (minimal epitope: FAILQDMRNT or AILQDMRNTI) (Maeda et al., 2004, 2005). The NC331–345 epitope is the same as the HTNV CD8$^+$ T cell epitope (ILQDMRNTI) identified in BALB/c mice. This sequence has also been shown to elicit a strong CTL response in humans (HLA-A2.1) who have been infected with HTNV and recovered (Lee et al., 2002). In addition, this region is highly conserved in all hantavirus prototypes, suggesting that this universal region may be important in eliciting hantavirus-specific T-cell responses.

In Puumala virus (PUUV) infection, N protein may be the dominant target of CD8$^+$ CTLs in infected patients (Van Epps et al., 2002). In immunization experiments using recombinant vaccinia viruses in a mouse model, both SNV N protein and especially HTNV N protein induced IFN-γ-producing cells (Maeda et al., 2004). Therefore, N seems to be a major CTL epitope. However, approximately 20% of all antigen-specific CD8$^+$ T cells were N-specific in our study (Fig. 1A), indicating that N is not the major epitope in BALB/c mice. Gn and Gc may be major target proteins of CD8$^+$ T cells in this mouse strain. Indeed, there are several reports of antigen-specific CD8$^+$ T cells being elicited not only by N, but also by Gn and Gc in patients with PUUV, SNV, and HTNV (Van Epps et al., 1999; Kilpatrick et al., 2004; Terajima et al., 2002).

The frequency of antigen-specific CD8$^+$ T cells may be related to pathogenic severity. In SNV infection, the frequency of SNV-specific CD8$^+$ T cells was significantly higher in patients with severe HPS (7.4–44.2%) than in patients with moderate HPS (2.9–9.8%) (Kilpatrick et al., 2004). Thus, virus-specific CD8$^+$ T cells may contribute to disease outcome. In the BALB/c mice used in this study, the total HTNV-specific CD8$^+$ T cell response itself is very low (less than 2%) compared to the response to other viruses (e.g., above 20% in lymphocytic choriomeningitis virus; Fig. 1) (Woo et al., 2005; Zhou et al., 2004). The low frequency of HTNV-specific CD8$^+$ T cells in mice seems to be related to asymptomatic infection.

We synthesized the HTNV-specific MHC tetramer NP335–343, derived from the HTNV epitope identified in BALB/c mice, to analyze epitope-specific CD8$^+$ T cells. Using this tetramer, we observed that epitope-specific CD8$^+$ T cells appeared soon after infection (day 7) in a transient infection model. This corresponded to the kinetics of IFN-γ-inducible CD8$^+$ T cells. These results suggest that the tetramer NP335–343 is a useful tool to analyze epitope-specific CD8$^+$ T cells and that the immune response is normal in the transient infection model. However, a low induction of N-specific CD8$^+$ T cells was observed in the persistent infection model. Although one peak in the appearance of NP335–343-specific CD8$^+$ T cells occurred just before viral antigen elimination (13 weeks), the level was quite low, even in the convalescent phase. Mice are also killed by HTNV infection when inoculated with HTNV on day 0 (Ebihara et al., 2000; Yoshimatsu et al., 1997). Persistent hantavirus infection in mice occurs only when they are inoculated with HTNV within 24 h of birth (Araki et al., 2004b). Viruses can readily proliferate in newborn mice because the immune response may be incomplete compared to adult mice. When spleen cells from immunocompetent BALB/c mice were passively transferred to SCID mice 14 days after infection, they permitted viral persistence and suppression of virus-specific CD8$^+$ T cells. However, when spleen cells from immunocompetent BALB/c mice were passively transferred to SCID mice on the day of infection, they expressed virus-specific CD8$^+$ T cells normally (Araki et al., 2004a). These results suggest that CTL production is dependent on the host environment and is regulated by the viral antigen. It is thought that suppression of epitope-specific CD8$^+$ T cell production in this persistent infection model is also caused by large amounts of viral antigen.

CTLs are an important host–defense mechanism against many viral infections, particularly for the clearance of virus-infected cells. N-specific CTLs are strongly regulated and suppressed in this persistently infected mouse model by an unknown mechanism. Both pathogenic and nonpathogenic hantaviruses infect primary human endothelial cells (Pensiero et al., 1992; Yanagihara and Silverman, 1990) and dendritic cells (Raftery et al., 2002), as well as other cell lines from many species. Although there are no reports to show the infected cells *in vivo* in mice, infected immune cells are thought to regulate

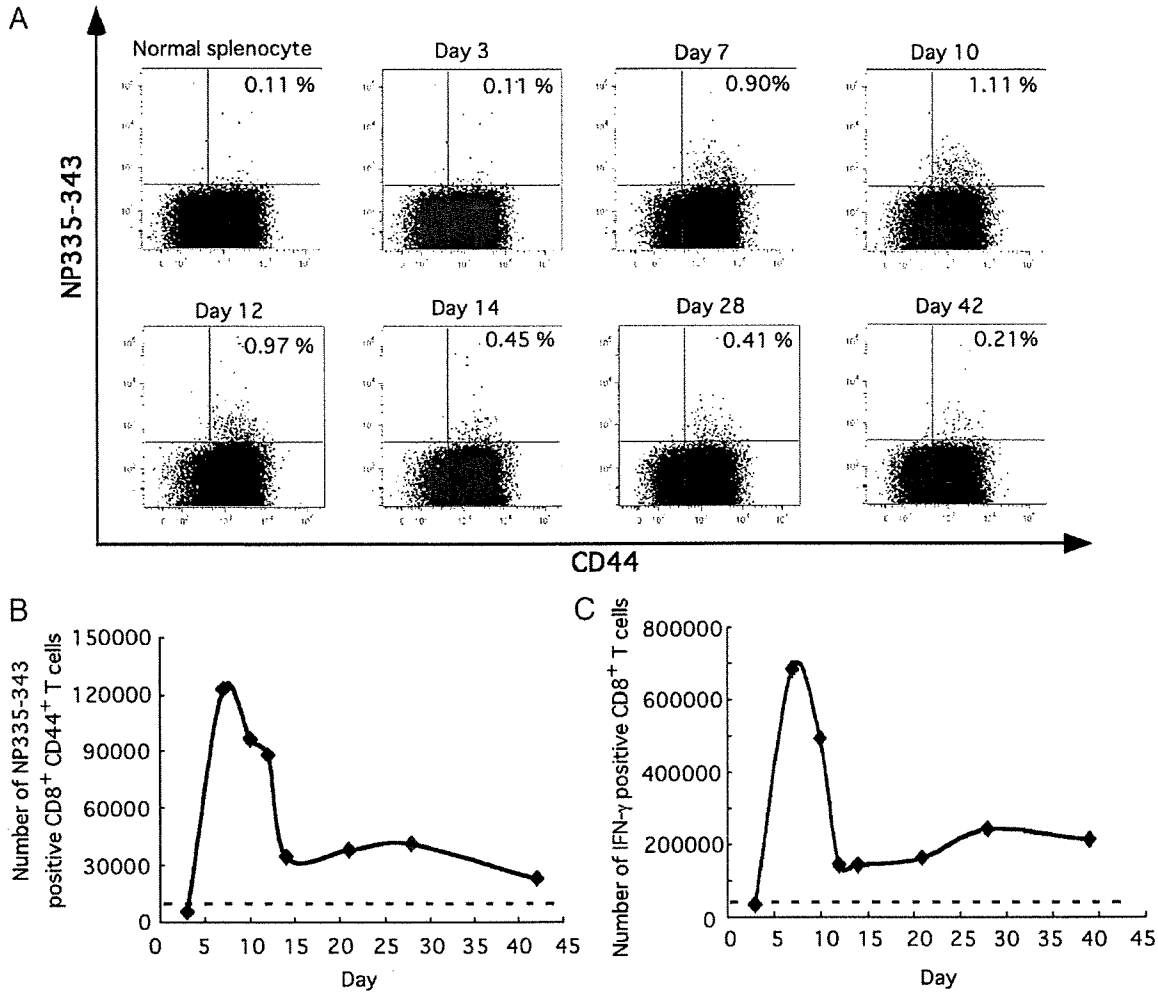

Fig. 3. Sequential analysis of NP335–343-specific $CD8^+$ T cells in a transient infection model. Spleen cells from normal adult mice and transiently infected adult mice, which were inoculated with HTNV cl-1, were stained with NP335–343. The number of $CD8^+$ T cells specific to the CTL epitope NP335–343 was determined by staining splenocytes with anti-CD8, anti-CD44, and MHC-I tetramer. (A) The dot plots are gated on total $CD8^+$ T cells, and the numbers are the percentages of tetramer-binding $CD8^+$ T cells of total $CD8^+$ T cells. (B) The representative percentage of $CD8^+$ T cells positive for NP335–343 is plotted over time following infection. The dotted line indicates the level of detection based on tetramer staining of splenocytes from naïve mice. (C) Spleen cells from BALB/c mice with or without HTNV infection were incubated with HTNV-infected P388D1 cells for 6 h in the presence of brefeldin A and IL-2. The representative percentage e of $CD8^+$ T cells producing IFN-γ is plotted over time following infection. The dotted line indicates the level of detection based on IFN-γ staining of splenocytes from naïve mice.

the alteration of these CTLs. We suspect that the alteration is triggered about 2 weeks after infection, as we have found that cells that strongly express N are detected only in the spleen of the model mice after 2 weeks of infection (unpublished data). Viral antigen is first detected in the spleen after infection (Yoshimatsu et al., 1997), and the change in CTLs occurs during this early phase. These infected cells may be immune cells, and we speculate that after infection they are involved in regulating immune responses, including the CTL response, and trigger persistent infection or viral pathogenesis. In conclusion, we demonstrated that major epitope-specific $CD8^+$ T cell production is strongly suppressed in a persistently infected mouse model. These two mouse models of transient and persistent infection are very useful for analyzing the immune response of virus-specific $CD8^+$ T cells with MHC tetramers. Using this method, further analyses should be performed to examine other protein-specific $CD8^+$ T cells, especially Gn and Gc. Although the molecular mechanism of this suppression requires further investigation, the strong suppression of the epitope-specific $CD8^+$ T cells in mice may be related to the induction of an asymptomatic infection. In particular, our findings may help improve therapies for patients with severe diseases controlled by $CD8^+$ T cells.

Materials and methods

Mice

All mice were treated according to the laboratory animal control guidelines of our institute, which conform to those of the

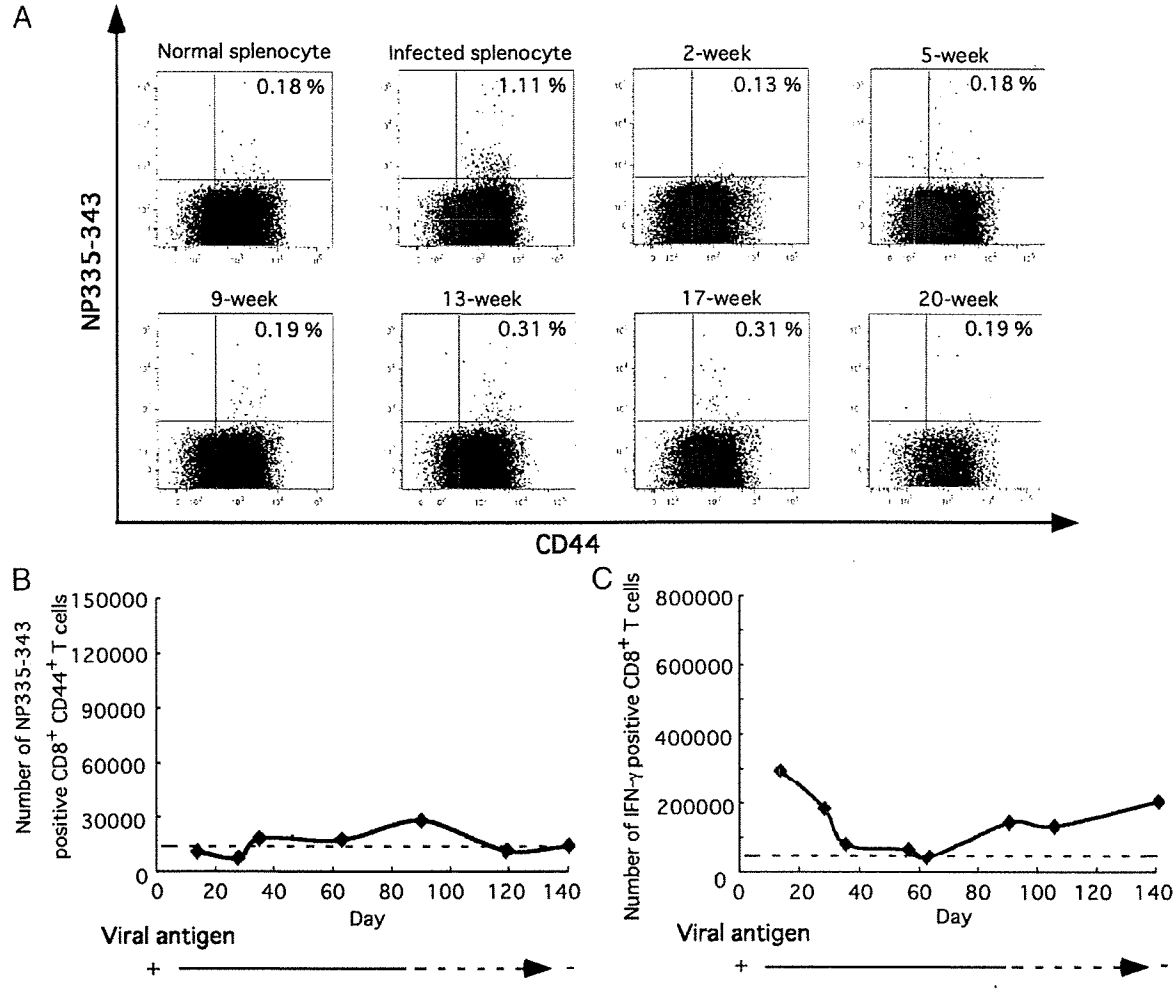

Fig. 4. Sequential analysis of NP335–343-specific $CD8^+$ T cells in a persistent infection model. BALB/c mice were inoculated with HTNV after birth (<24 h) and killed after several weeks. "Infected" indicates adult BALB/c mice that were inoculated with HTNV and recovered (positive controls). "Uninfected" denotes normal BALB/c mice (negative controls). (A) The dot plots are gated on total $CD8^+$ T cells, and the numbers are the percentages of tetramer-binding $CD8^+$ T cells of total $CD8^+$ T cells. (B) The representative percentage of $CD8^+$ T cells positive for NP335–343 is plotted over time following infection. The dotted line indicates the level of detection based on tetramer staining of splenocytes from naïve mice. (C) Spleen cells from BALB/c mice with or without HTNV infection were incubated with HTNV-infected P388D1 cells for 6 h in the presence of brefeldin A and IL-2. The representative percentage of $CD8^+$ T cells producing IFN-γ is plotted over time following infection. The dotted line indicates the level of detection based on IFN-γ staining of splenocytes from naïve mice.

U.S. National Institutes of Health (Bethesda, MD). Pregnant, 5-week-old female BALB/c mice were obtained from SLC (Hamamatsu, Japan). All experiments were performed in a class P3 facility.

Virus and viral infection of mice

HTNV cl-1 was obtained by plaque cloning from the HTNV strain 76–118 (Ebihara et al., 2000). The virus was propagated in the E6 clone of the Vero cell line (ATCC c1008) in Eagle's minimal essential medium (EMEM; Invitrogen, Carlsbad, CA), supplemented with 5% fetal bovine serum (FBS). We used two series of infected mice. For the production of persistently infected mice, BALB/c mice were subcutaneously (s.c.) inoculated with 1.3 focus-forming units (FFU) of HTNV within 24 h of birth (1.3 FFU=0.1 $NMLD_{50}$ [50% newborn mouse lethal dose]). For the production of transiently infected mice, adult (more than 5 weeks old) mice were intraperitonially inoculated with 160,000 FFU of HTNV.

Cells

The murine macrophage-like cell line P388D1 ($H\text{-}2^d$) was cultured in RPMI 1640 medium (Sigma, St. Louis, MO), supplemented with 5% FBS and 2-mercaptoethanol (2-ME, 50 μM). P388D1 cells continuously infected with HTNV were prepared as antigen-presenting cells, as described previously (Araki et al., 2003). Single-cell suspensions of spleen cells were obtained by homogenizing spleens in RPMI 1640 medium, supplemented with 10% FBS and 2-ME (50 μM). Erythrocytes were lysed with ACT solution (0.83% NH_4Cl).

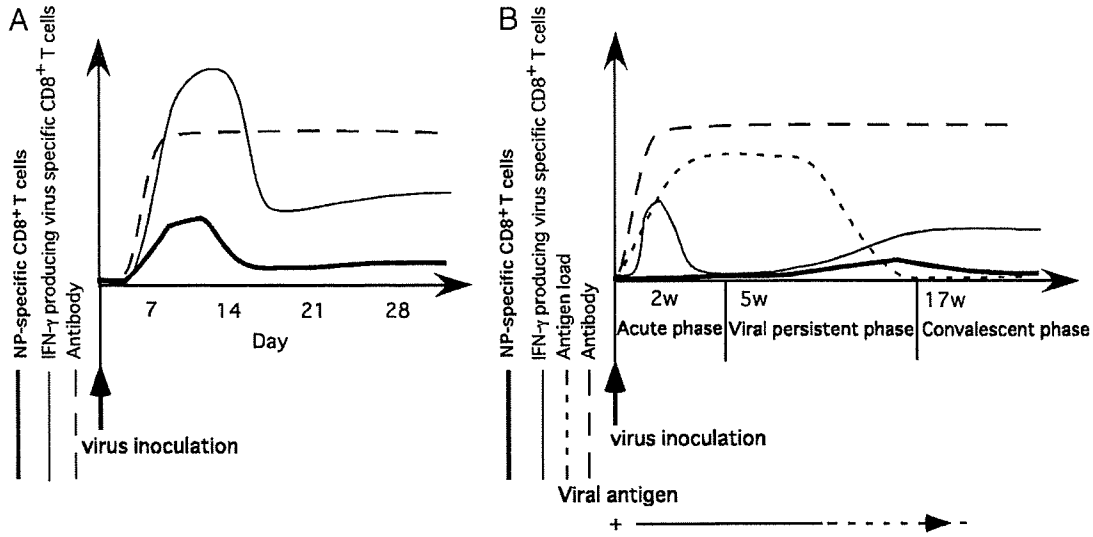

Fig. 5. Schema showing fluctuations in the numbers of $CD8^+$ T cells producing IFN-γ or that are positive for NP335–343, neutralizing antibodies titers, and antigen loads (amounts of N protein in lungs) in HTNV-infected adult or newborn mice based on data from the literature (Araki et al., 2003). (A) In transiently infected mice, NP335–343-positive $CD8^+$ T cells were normally expressed soon after infection, suggesting that transiently infected mice have normal immune responses. (B) In persistently infected mice, IFN-γ-producing virus-specific $CD8^+$ T cells were induced in the acute and convalescent phases. However, typical NP335–343-positive $CD8^+$ T cells were not detected at all time points. These results suggest that NP335–343-positive $CD8^+$ T cells were suppressed by a viral antigen.

Peptides and other reagents

Overlapping 15-mer peptides ($n=105$) with 10-amino acid overlaps, spanning residues 1–430 of the HTNV nucleocapsid protein (N), based on strain 76–118, and seven overlapping 11-mer peptides with 9-amino acid overlaps, spanning residues 329–347 of N, were purchased from Mimotope (Melbourne, Australia) and Hokkaido System Science (Sapporo, Japan). The nonamer peptide ILQDMRNTI, which was identified as the sequence of a CTL epitope, was purchased as a highly purified product from Hokkaido System Science. Stock solutions of these synthetic peptides were prepared in 100% DMSO at concentrations of 2 mg/mL for the 15-mer and 11-mer peptides and 5 mg/mL for the nonamer peptide. All were diluted to 0.2 μg/mL before use for *in vitro* stimulation. Goat anti-mouse H-$2D^d$ antibody (34-2-12) and goat anti-mouse H-$2K^d$ antibody (SF1-1.1) were purchased from BD Biosciences (Franklin Lakes, NJ) and were used for the inhibition-of-peptide-stimulation assay. The H-$2K^d$-restricted class-I peptide tetramer from the sequence ILQDMRNTI named NP335–343 was synthesized at the NIH Tetramer Facility.

IFN-γ staining for peptide screening

To detect intracellular gamma interferon (IFN-γ), spleen cells were added to 96-well V-bottomed plates at a concentration of 1×10^6 cells/well in RPMI 1640 medium, supplemented with 10% FBS, 2-ME (50 μM), murine recombinant interleukin-2 (IL-2; 40 ng/mL, Sigma), and brefeldin A (10 μg/mL, Sigma), along with peptide or HTNV-infected or uninfected P388D1 cells. The P388D1 cells were co-cultured at a concentration of 5×10^5 cells/well with the spleen cells. Peptide was added at a concentration of 0.1 to 0.2 μg/mL to the spleen cell cultures. After a 6-h incubation, cells were suspended in phosphate-buffered saline (PBS) and transferred to a 96-well plate containing ethidium monoazide bromide (EMA; 5 μg/mL, Invitrogen). After a 15-min incubation on ice in the dark, cells were washed with PBS twice and exposed to light for 10 min. Cells were washed with FACS buffer (PBS containing 1% bovine serum albumin [BSA] and 0.1% NaN_3) and stained with the anti-CD8a PE (Ly-2) antibody (eBioscience, San Diego, CA) for 30 min on ice. Cells were then washed with FACS buffer and fixed with 2% paraformaldehyde–PBS. After a 20-min incubation at room temperature, the cells were washed with FACS buffer, resuspended in permeation buffer (PBS containing 0.5% BSA, 0.5% saponin [Sigma], 0.1% NaN_3), and incubated for 10 min at room temperature. The cells were then stained with fluorescein isothiocyanate-conjugated rat anti-mouse IFN-γ antibody (Caltag Laboratories, San Francisco, CA), incubated for 30 min at room temperature, and washed twice with permeation buffer. Cells were then given a final wash with FACS buffer before analysis. Cells were analyzed using a FACS Calibur (Becton Dickinson, Franklin Lakes, NJ) and data analysis was conducted using FlowJo software (Tree Star, San Carlos, CA).

Inhibition-of-peptide-stimulation assay

Spleen cells were added to 96-well V-bottomed plates at a concentration of 1×10^6 cells/well in RPMI 1640 medium, supplemented with 10% FBS, 2-ME (50 μM), murine recombinant interleukin-2 (IL-2; 40 ng/mL, Sigma), and brefeldin A (10 μg/mL, Sigma). The NP335–343 peptide was added at a concentration of 0.2 μg/mL with or without anti-H-$2D^d$ or anti H-$2K^d$ antibodies (50 μg/mL). To remove sodium azide from the antibodies, immediately before the assay they

were dialyzed for 3 h in PBS using a microdialyzer Toru-kun (NIPPON Genetics, Tokyo). After a 6-h incubation, IFN-γ staining was carried out using the method described above.

Tetramer staining and flow cytometry

Spleen cells in several phases were stained, as described below. Cells (1×10^6 per well) were suspended in PBS and transferred to a 96-well plate containing EMA (5 μg/mL). After a 15-min incubation on ice in the dark, cells were washed with PBS twice and exposed to light for 10 min. The cells were washed with FACS buffer and stained with the anti-CD8a APC and -CD44 FITC antibodies (eBioscience) for 30 min on ice. After washing with FACS buffer, cells were stained with NP335–343 at a 1:500 dilution for 30 min at room temperature. Cells were then washed with FACS buffer and fixed with 2% paraformaldehyde–PBS. Tetramer-positive $CD44^+$ cells were analyzed with gates set on EMA-negative and CD8-positive cells. The cell samples were examined using a FACS Canto (Becton Dickinson), and data analysis was conducted with FACS Diva software (Becton Dickinson).

Acknowledgments

We thank the NIH Tetramer Facility (Atlanta, GA) for providing us with the ILQDMRNTI/H-$2K^d$ tetramer. This work was supported in part by a grant from the 21st Century COE Program, "Program of Excellence for Zoonosis Control," and in part by Grants-in-Aid for Scientific Research and the Development of Science from the Ministry of Education, Culture, Sports, Science, and Technology, Japan.

The English in this document has been checked by at least two professional editors, both native speakers of English. For a certificate, see: http://www.textcheck.com/cgi-bin/certificate.cgi?id=5X40nv.

References

Araki, K., Yoshimatsu, K., Lee, B.H., Kariwa, H., Takashima, I., Arikawa, J., 2003. Hantavirus-specific CD8(+)-T-cell responses in newborn mice persistently infected with Hantaan virus. J. Virol. 77 (15), 8408–8417.

Araki, K., Yoshimatsu, K., Lee, B.H., Kariwa, H., Takashima, I., Arikawa, J., 2004a. A new model of Hantaan virus persistence in mice: the balance between HTNV infection and CD8(+) T-cell responses. Virology 322 (2), 318–327.

Araki, K., Yoshimatsu, K., Lee, B.H., Okumura, M., Kariwa, H., Takashima, I., Arikawa, J., 2004b. Age-dependent hantavirus-specific CD8(+) T-cell responses in mice infected with Hantaan virus. Arch. Virol. 149 (7), 1373–1382.

Carey, D.E., Reuben, R., Panicker, K.N., Shope, R.E., Myers, R.M., 1971. Thottapalayam virus: a presumptive arbovirus isolated from a shrew in India. Indian J. Med. Res. 59 (11), 1758–1760.

Chen, L.B., Yang, W.S., 1990. Abnormalities of T cell immunoregulation in hemorrhagic fever with renal syndrome. J. Infect. Dis. 161 (5), 1016–1019.

Ebihara, H., Yoshimatsu, K., Ogino, M., Araki, K., Ami, Y., Kariwa, H., Takashima, I., Li, D., Arikawa, J., 2000. Pathogenicity of Hantaan virus in newborn mice: genetic reassortant study demonstrating that a single amino acid change in glycoprotein G1 is related to virulence. J. Virol. 74 (19), 9245–9255.

Huang, C., Jin, B., Wang, M., Li, E., Sun, C., 1994. Hemorrhagic fever with renal syndrome: relationship between pathogenesis and cellular immunity. J. Infect. Dis. 169 (4), 868–870.

Kilpatrick, E.D., Terajima, M., Koster, F.T., Catalina, M.D., Cruz, J., Ennis, F.A., 2004. Role of specific CD8+ T cells in the severity of a fulminant zoonotic viral hemorrhagic fever, hantavirus pulmonary syndrome. J. Immunol. 172 (5), 3297–3304.

Lednicky, J.A., 2003. Hantaviruses. A short review. Arch. Pathol. Lab. Med. 127 (1), 30–35.

Lee, H.W., van der Groen, G., 1989. Hemorrhagic fever with renal syndrome. Prog. Med. Virol. 36, 62–102.

Lee, K.Y., Chun, E., Kim, N.Y., Seong, B.L., 2002. Characterization of HLA-A2.1-restricted epitopes, conserved in both Hantaan and Sin Nombre viruses, in Hantaan virus-infected patients. J. Gen. Virol. 83 (Pt 5), 1131–1136.

Maeda, K., West, K., Toyosaki-Maeda, T., Rothman, A.L., Ennis, F.A., Terajima, M., 2004. Identification and analysis for cross-reactivity among hantaviruses of H-2b-restricted cytotoxic T-lymphocyte epitopes in Sin Nombre virus nucleocapsid protein. J. Gen. Virol. 85 (Pt 7), 1909–1919.

Maeda, K., West, K., Hayasaka, D., Ennis, F.A., Terajima, M., 2005. Recombinant adenovirus vector vaccine induces stronger cytotoxic T-cell responses than recombinant vaccinia virus vector, plasmid DNA, or a combination of these. Viral. Immunol. 18 (4), 657–667.

Mata, M., Travers, P.J., Liu, Q., Frankel, F.R., Paterson, Y., 1998. The MHC class I-restricted immune response to HIV-gag in BALB/c mice selects a single epitope that does not have a predictable MHC-binding motif and binds to Kd through interactions between a glutamine at P3 and pocket D. J. Immunol. 161 (6), 2985–2993.

Meyer, B.J., Schmaljohn, C.S., 2000. Persistent hantavirus infections: characteristics and mechanisms. Trends Microbiol. 8 (2), 61–67.

Mustonen, J., Helin, H., Pietila, K., Brummer-Korvenkontio, M., Hedman, K., Vaheri, A., Pasternack, A., 1994. Renal biopsy findings and clinicopathologic correlations in nephropathia epidemica. Clin. Nephrol. 41 (3), 121–126.

Nolte, K.B., Feddersen, R.M., Foucar, K., Zaki, S.R., Koster, F.T., Madar, D., Merlin, T.L., McFeeley, P.J., Umland, E.T., Zumwalt, R.E., 1995. Hantavirus pulmonary syndrome in the United States: a pathological description of a disease caused by a new agent. Hum. Pathol. 26 (1), 110–120.

Ogino, M., Yoshimatsu, K., Ebihara, H., Araki, K., Lee, B.H., Okumura, M., Arikawa, J., 2004. Cell fusion activities of Hantaan virus envelope glycoproteins. J. Virol. 78 (19), 10776–10782.

Park, J.M., Cho, S.Y., Hwang, Y.K., Um, S.H., Kim, W.J., Cheong, H.S., Byun, S.M., 2000. Identification of H-2K(b)-restricted T-cell epitopes within the nucleocapsid protein of Hantaan virus and establishment of cytotoxic T-cell clones. J. Med. Virol. 60 (2), 189–199.

Parker, K.C., Bednarek, M.A., Coligan, J.E., 1994. Scheme for ranking potential HLA-A2 binding peptides based on independent binding of individual peptide side-chains. J. Immunol. 152 (1), 163–175.

Pensiero, M.N., Sharefkin, J.B., Dieffenbach, C.W., Hay, J., 1992. Hantaan virus infection of human endothelial cells. J. Virol. 66 (10), 5929–5936.

Raftery, M.J., Kraus, A.A., Ulrich, R., Kruger, D.H., Schonrich, G., 2002. Hantavirus infection of dendritic cells. J. Virol. 76 (21), 10724–10733.

Temonen, M., Mustonen, J., Helin, H., Pasternack, A., Vaheri, A., Holthofer, H., 1996. Cytokines, adhesion molecules, and cellular infiltration in nephropathia epidemica kidneys: an immunohistochemical study. Clin. Immunol. Immunopathol. 78 (1), 47–55.

Terajima, M., Van Epps, H.L., Li, D., Leporati, A.M., Juhlin, S.E., Mustonen, J., Vaheri, A., Ennis, F.A., 2002. Generation of recombinant vaccinia viruses expressing Puumala virus proteins and use in isolating cytotoxic T cells specific for Puumala virus. Virus Res. 84 (1–2), 67–77.

Van Epps, H.L., Schmaljohn, C.S., Ennis, F.A., 1999. Human memory cytotoxic T-lymphocyte (CTL) responses to Hantaan virus infection: identification of virus-specific and cross-reactive CD8(+) CTL epitopes on nucleocapsid protein. J. Virol. 73 (7), 5301–5308.

Van Epps, H.L., Terajima, M., Mustonen, J., Arstila, T.P., Corey, E.A., Vaheri, A., Ennis, F.A., 2002. Long-lived memory T lymphocyte responses after hantavirus infection. J. Exp. Med. 196 (5), 579–588.

Woo, G.J., Chun, E.Y., Kim, K.H., Kim, W., 2005. Analysis of immune responses against nucleocapsid protein of the Hantaan virus elicited by virus infection or DNA vaccination. J. Microbiol. 43 (6), 537–545.

Yanagihara, R., Silverman, D.J., 1990. Experimental infection of human vascular endothelial cells by pathogenic and nonpathogenic hantaviruses. Arch. Virol. 111 (3–4), 281–286.

Yoshimatsu, K., Arikawa, J., Ohbora, S., Itakura, C., 1997. Hantavirus infection in SCID mice. J. Vet. Med. Sci. 59 (10), 863–868.

Zaki, S.R., Greer, P.W., Coffield, L.M., Goldsmith, C.S., Nolte, K.B., Foucar, K., Feddersen, R.M., Zumwalt, R.E., Miller, G.L., Khan, A.S., et al., 1995. Hantavirus pulmonary syndrome. Pathogenesis of an emerging infectious disease. Am. J. Pathol. 146 (3), 552–579.

Zhou, S., Ou, R., Huang, L., Price, G.E., Moskophidis, D., 2004. Differential tissue-specific regulation of antiviral CD8+ T-cell immune responses during chronic viral infection. J. Virol. 78 (7), 3578–3600.

CLINICAL AND VACCINE IMMUNOLOGY, Sept. 2007, p. 1182–1189 Vol. 14, No. 9
1556-6811/07/$08.00+0 doi:10.1128/CVI.00101-07

Development of Recombinant Nucleoprotein-Based Diagnostic Systems for Lassa Fever[▽]

Masayuki Saijo,[1]*† Marie-Claude Georges-Courbot,[2] Philippe Marianneau,[2] Victor Romanowski,[3] Shuetsu Fukushi,[1] Tetsuya Mizutani,[1] Alain-Jean Georges,[4] Takeshi Kurata,[5] Ichiro Kurane,[1] and Shigeru Morikawa[1]†

Department of Virology 1, National Institute of Infectious Diseases, 4-7-1 Gakuen, Musashimurayama, Tokyo 208-0011, Japan[1]; Unit of Biology of Viral Emerging Infections, Institute Pasteur, IFR 128 Biosciences Lyon-Gerland, 21 Avenue Tony Garnier, 69365 Lyon Cedex 07, France[2]; Instituto de Bioquímica y Biologíca Molecular, Facultad de Ciencias Exactas, Universidad Nacional de a Plata, 1900 La Plata, Argentina[3]; Laboratory P4 Jean-Merieux-INSERM, 21 Avenue Tony Garnier 69365 Lyon Cedex 07, France[4]; and Department of Pathology, National Institute of Infectious Diseases, 1-23-1 Toyama, Shinjuku-ku, Tokyo 162-864, Japan[5]

Received 1 March 2007/Returned for modification 22 April 2007/Accepted 20 June 2007

Diagnostic systems for Lassa fever (LF), a viral hemorrhagic fever caused by Lassa virus (LASV), such as enzyme immunoassays for the detection of LASV antibodies and LASV antigens, were developed using the recombinant nucleoprotein (rNP) of LASV (LASV-rNP). The LASV-rNP was expressed in a recombinant baculovirus system. LASV-rNP was used as an antigen in the detection of LASV-antibodies and as an immunogen for the production of monoclonal antibodies. The LASV-rNP was also expressed in HeLa cells by transfection with the expression vector encoding cDNA of the LASV-NP gene. An immunoglobulin G enzyme-linked immunosorbent assay (ELISA) using LASV-rNP and an indirect immunofluorescence assay using LASV-rNP-expressing HeLa cells were confirmed to have high sensitivity and specificity in the detection of LASV-antibodies. A novel monoclonal antibody to LASV-rNP, monoclonal antibody 4A5, was established. A sandwich antigen capture (Ag-capture) ELISA using the monoclonal antibody and an anti-LASV-rNP rabbit serum as capture and detection antibodies, respectively, was then developed. Authentic LASV nucleoprotein in serum samples collected from hamsters experimentally infected with LASV was detected by the Ag-capture ELISA. The Ag-capture ELISA specifically detected LASV-rNP but not the rNPs of lymphocytic choriomeningitis virus or Junin virus. The sensitivity of the Ag-capture ELISA in detecting LASV antigens was comparable to that of reverse transcription-PCR in detecting LASV RNA. These LASV rNP-based diagnostics were confirmed to be useful in the diagnosis of LF even in institutes without a high containment laboratory, since the antigens can be prepared without manipulation of the infectious viruses.

Lassa fever (LF) is a viral hemorrhagic fever caused by Lassa virus (LASV), an Old World arenavirus. Many cases of LF occur in western Africa in countries such as Guinea, Sierra Leone, and Nigeria (7, 23, 27, 29–31). It is thought that LASV infects tens of thousands of humans annually and causes hundreds to thousands of deaths (34). Humans become infected through contact with infected excreta, tissue, or blood from the peridomestic rodent, *Mastomys natalensis*, the reservoir host of LASV (34). LASV can be transmitted to other humans via mucosal or cutaneous contact or through nosocomial contamination (27). More than 20 imported cases of LF have been reported outside the endemic region in areas such as the United States, Canada, Europe, and Japan (1, 2, 13, 15, 18, 24, 25). Recently, the potential for the use of hemorrhagic fever viruses, including LASV, as a biological weapon has been emphasized (5, 6). Therefore, the development of diagnostic systems for LF is important even in countries free from LF outbreaks to date.

Manipulation of infectious LASV is necessary for the detection of specific antibodies. However, a high-containment laboratory (biosafety level 4 [BSL-4]) is required for handling infectious LASV and, therefore, the preparation of LASV antigens cannot be implemented in institutes without a BSL-4 facility. Within this framework, it is important to develop sensitive and specific diagnostic systems for LF that eliminate the need for the manipulation of infectious LASV. In the present study, the recombinant nucleoprotein (rNP) of LASV (LASV-rNP) was expressed and evaluated for its ability to detect LASV antibodies. LASV-rNP-based enzyme-linked immunosorbent and indirect immunofluorescence assays (ELISA and IIFA) were developed. Furthermore, novel monoclonal antibodies to LASV-rNP were generated and used in combination with the recombinant antigen to develop an LASV antigen (nucleoprotein) capture ELISA. The present study presents an alternative strategy to develop diagnostic systems without handling infectious LASV.

MATERIALS AND METHODS

Cells. A HeLa cell line was cultured in the Eagle minimum essential medium supplemented with 10% fetal bovine serum and the antibiotics penicillin G and streptomycin (MEM-10FBS). Tn5 insect cells were used for the expression of the rNPs of arenaviruses (LASV, lymphocytic choriomeningitis virus [LCMV], and Junin virus [JUNV]) in a baculovirus system. The Tn5 insect cells were cultured as reported previously (38).

* Corresponding author. Mailing address: Special Pathogens Laboratory, Department of Virology 1, National Institute of Infectious Diseases, 4-7-1 Gakuen, Musashimurayama, Tokyo 208-0011, Japan. Phone: 81-42-561-0771, ext. 320. Fax: 81-42-561-2039. E-mail: msaijo@nih.go.jp.
† M.S. and S.M. contributed equally to this study.
▽ Published ahead of print on 18 July 2007.

Viruses. LASV (strain AV), which was isolated from an imported case of LF to Germany from West Africa, was used (13). The experimental process that required manipulation of infectious LASV was carried out in the BSL-4 laboratory in the P4 laboratory, INSERM, Lyon, France. Mopeia virus (MOPV), which belongs to the family *Arenaviridae*, genus *Arenavirus*, was also used. Recombinant NPs of LCMV (26) and JUNV (11), designated LCMV-rNP and JUNV-rNP, respectively, were also expressed in a baculovirus system and used in the study. A baculovirus (Ac-ΔP), which lacks polyhedrin expression, was used as a control virus (26). The virus titer of LASV in serum samples was determined by using a focus-forming unit (FFU) assay as described previously (3).

Sera. Four human serum samples—three samples serially collected from one patient with LF and one additional sample from another patient with LF—and ninety-six human sera collected from Japanese subjects with no history of travel to areas where LF is endemic were used as positive and negative controls, respectively. The patient with LF, from whom three serial serum samples were collected, was the first case of LF to be imported in Japan in 1987 (15). The other human serum sample was provided from the Special Pathogens Branch, National Center for Infectious Diseases, Centers for Disease Control and Prevention, Atlanta, GA.

Serum samples collected from five monkeys (*Macaca fascicularis*) subcutaneously infected with LASV strain AV at 10^3 FFU (two monkeys) or 10^7 FFU (three monkeys) and those collected from four monkeys with mock infection were also used. The serum samples used in the study were collected at 4 to 5 weeks postchallenge.

Five hamsters were subcutaneously infected with 10^3 FFU of LASV, strain AV, and blood was drawn on days 0, 4, 11, and 16 postinfection, taking the day on which the virus was inoculated as day 0. Serum fractions of the collected blood specimens were separated and tested for LASV antigen by antigen capture (Ag-capture) ELISA and reverse transcription-PCR (RT-PCR).

Rabbit sera (polyclonal antibodies) were raised against LASV-rNP, LCMV-rNP, and JUNV-rNP by immunization of rabbits with the purified LASV-rNP, LCMV-rNP, and JUNV-rNP, respectively, in the form of a mixture with the adjuvant, Inject Alum (Pierce). Rabbits were immunized with sufficient amount of the purified nucleoproteins of each virus three times with an interval of 2 weeks. After confirmation of the increased titer, >10,000 times as determined by indirect immunofluorescence assay, which was developed in the present study, blood was drawn from the rabbits, and the serum fraction was used in the present study.

Recombinant baculovirus. In order to construct the transfer vector, a cDNA clone of NP from LASV strain Josiah was used. The cDNA was kindly provided by J. B. McCormick, former Director of the Special Pathogens Branch, National Centers for Infectious Diseases, Centers for Disease Control and Prevention. The complete nucleotide sequence of the NP gene is registered in GenBank under the accession number NC_004296. The DNA of the LASV-NP was amplified by PCR from the source using the primers LAS-NfB (5′-GTGGATCCA ACACAACAATCTGG-3′; the BamHI restriction site is underlined) and LAS-NrB (5′-CCGGATCCATTTACAGAACGACTC-3′). The PCR conditions were the same as previously reported (38). The 1,743-bp amplification product was digested with BamHI and subcloned into the BamHI site of pQE32 vector DNA (QIAGEN GmbH, Hilden, Germany) to construct pQE32-LASV-NP. The inserted LASV-NP DNA was sequenced by using appropriate primers with an ABI Prism 310 genetic analyzer (PE Applied Biosystems, Foster City, CA) and confirmed to be in proper orientation downstream the promoter and identical to the original sequence. The DNA fragment of LASV-NP with a histidine (His) tag was isolated from the plasmid, pQE32-LASV-NP, by digestion with EcoRI and HindIII. It was then blunt repaired with Klenow enzyme and ligated into the blunt-ended BamHI site of pAcYM1 (26). The resulting recombinant transfer vector with the correct orientation with respect to the polyhedrin promoter was constructed (pACYM1-His-LASV-NP). Tn*5* insect cells were transfected with mixtures of purified *Autographa californica* nuclear polyhedrosis virus (AcMNPV) DNA and pAcYM1-His-LASV-NP according to the procedures described by Kitts et al. (20), with the modification of Matsuura et al. (26). Recombinant baculovirus was then isolated. The baculovirus, which expressed His-tagged LASV-rNP (His-LASV-rNP), was designated Ac-His-LASV-NP.

The baculovirus, Ac-LCMV-NP, which expressed LCMV-rNP, was used in the study (26).

The recombinant baculovirus that expressed JUNV-rNP, Ac-JUNV-NP, was generated as follows. The gene encoding the NP of JUNV (strain MC2) was reconstructed from cloned cDNA. The nucleotide sequence of the interest gene was deposited in GenBank under accession number D10072 (12). A complete NP gene with the initiation and stop codons amplified by PCR using appropriate primers, which possessed BamHI restriction sites. The entire DNA product of JUNV-NP was digested with BamHI and ligated into the transfer vector pAcUW2B (28). Clones containing the insert in the correct orientation were selected, and the plasmid DNA was used for cotransfection in Sf21 cells with a polyhedrin-positive AcMNPV DNA, and the supernatant culture was screened for a polyhedrin-negative phenotype by plaque assay (19). Finally, recombinant baculovirus clones overexpressing JUNV-rNP were obtained after three successive plaque purifications. One of them, designated AcNMPV-Jun-N122, was used in the present study and is referred to hereafter as Ac-JUNV-NP.

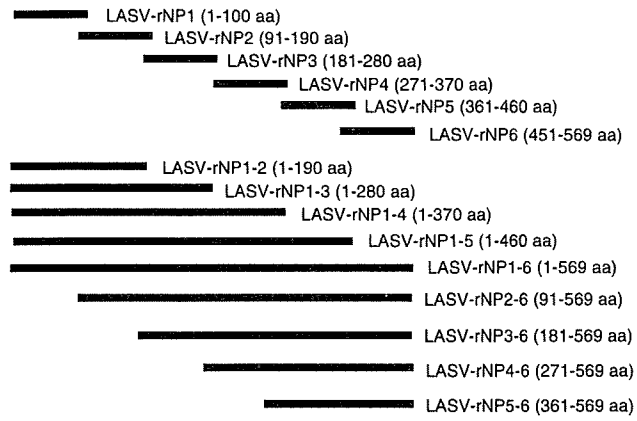

FIG. 1. Schematic representation of truncated LASV-rNP expressed as a form of GST fusion protein in *E. coli* transformed with the corresponding expression vector. The description "LASV-NP1-6" in the middle portion of the figure indicates full-length LASV-rNP.

Expression and purification of His-LASV-rNP, LCMV-rNP, and JUNV-rNP. Tn*5* cells infected with Ac-His-LASV-NP were incubated at 26°C for 72 h. The cells were then washed twice with cold phosphate-buffered saline (PBS) solution. A preliminary study demonstrated that most of the Tn*5* cellular proteins were solubilized in PBS containing 2 M urea (PBS–2 M urea) but that the His-LASV-rNP was insoluble and that the LASV-rNP could be solubilized in PBS containing 8 M urea (PBS–8 M urea). Therefore, the Tn*5* cells infected with Ac-His-LASV-NP were first suspended in PBS–2 M urea. After the centrifugation of the cell suspensions at 15,000 × *g* for 10 min, the pellet fractions were collected and then were solubilized in PBS–8 M urea. After the centrifugation of the samples, the supernatant fractions were used as the purified antigens. LCMV-rNP and JUNV-rNP showed dissolution characteristics in urea similar to those of His-LASV-rNP; therefore, LCMV-rNP and JUNV-rNP were also fractioned in the same way as the His-LASV-rNP. The control antigen was produced from Tn*5* cells infected with Ac-ΔP in the same manner as that for the positive antigens. The His-LASV-rNP was also purified by using the Ni^{2+} column purification method as reported previously (38). The source for His-LASV-rNP-purification was the supernatant fraction of the PBS–8 M urea-treated Tn*5* cells infected with Ac-His-LASV-NP after sufficient dilution with PBS in order to reduce the urea concentration.

SDS-PAGE. The expression and purification efficiency of His-LASV-rNP, LCMV-rNP, and JUNV-rNP were analyzed on sodium dodecyl sulfate-polyacrylamide gel electrophoresis (SDS-PAGE) gels (12% polyacrylamide) after staining with Coomassie blue.

Establishment of MAbs. Monoclonal antibodies (MAbs) were generated as previously described (32, 41). BALB/c mice were immunized with purified His-LASV-rNP in the present study. Isotypes of the MAbs were determined by using a mouse MAb isotyping kit (Life Technologies).

Expression of truncated NPs of LASV. In order to determine the epitope of the MAbs to the His-LASV-rNP, truncated LASV-rNPs were expressed as a form of fusion protein with glutathione *S*-transferase (GST) as shown in Fig. 1. The DNA corresponding to each of the truncated NP fragments was amplified with the designed primers. The amplified DNA was subcloned into the BamHI and EcoRI cloning sites of plasmid pGEX-2T (Amersham Pharmacia Biotech, Buckinghamshire, England). Each insert was sequenced and confirmed to be in the correct frame and identical to the original sequence. The GST-tagged nucleoprotein fragments were expressed in an *Escherichia coli* BL21 system.

Western blotting. The MAbs were tested for reactivity to His-LASV-rNP and its fragments by Western blotting as reported previously (17, 32, 41).

Pepscan analyses. ELISA was performed as reported previously with the purified rNP or partial nucleoprotein peptides as the antigen (33). The peptides

FIG. 2. SDS-PAGE analyses of the purification of His-LASV-rNP using the Ni^{2+} column purification method (A) and of the semipurification strategy based on the hydrophobic property of arenavirus nucleoproteins (B). The supernatant fractions of the Ac-ΔP-, Ac-His-LASV-NP-, Ac-LCMV-NP-, or Ac-JUNV-NP-infected Tn*5* cells treated with PBS–2 M urea (B, left part) are shown. The pellet fractions of these cells treated with PBS–2 M urea were further solubilized with PBS–8 M urea (B, right part).

were shifted by 1 amino acid (aa), with a consecutive overlap of 9 aa to cover the entire LASV-NP1 (aa 1 to 100) and LASV-NP5 (aa 361 to 460) fragments. Linear epitopes on the NP were determined by using Pepscan (Chiron Technologies, Clayton, Australia) according to the manufacturer's instructions. Ninety-six peptides were prepared as 14-aa biotinylated peptides, including a 4-aa spacer sequence (SGSG) at the amino-terminal end, according to each of the amino acid sequences of the LASV-rNP1 and LASV-rNP5 of the LASV Josiah strain. The methods were previously described in detail (33).

IgG-ELISA. Immunoglobulin G (IgG)-ELISA was performed as previously described except for the antigen preparation (38, 39). Briefly, ELISA plates (96-well type plate, Pro-Bind; Falcon; Becton Dickinson Labware, Franklin Lakes, NJ) were coated with the predetermined optimal quantity of purified His-LASV-rNP, LCMV-rNP, or JUNV-rNP (approximately 100 ng/well) at 4°C overnight. Then, each well of the plates was inoculated with 200 μl of PBS containing 5% skim milk and 0.05% Tween 20 (M-T-PBS), followed by incubation for 1 h for blocking. The plates were washed three times with T-PBS and then inoculated with the test samples (100 μl/well), which were diluted fourfold from 1:100 to 1:6,400 with M-T-PBS. After a 1-h incubation period, the plates were washed three times with T-PBS, and then the plates were inoculated with goat anti-human IgG antibody labeled with HRPO (1:1,000 dilution; Zymed Laboratory). After a further 1-h incubation period, the plates were washed and 100 μl of ABTS [2,2'azinobis(3-ethylbenzthiazolinesulfonic acid)] solution (Roche Diagnostics, Mannheim, Germany) was added to each well. The plates were incubated for 30 min at room temperature, and optical density was at 405 nm (OD_{405}) was measured against a reference of 490 nm. The adjusted OD_{405} was calculated by subtracting the OD of the negative antigen-coated wells from that of the corresponding wells. The means and standard deviations were calculated from the 96 control sera. The cutoff value for the assay was defined as the mean plus 3 standard deviations.

Immunofluorescence. The pQE32-LASV-NP was digested with BamHI, and the insert was subcloned into the BamHI site of the pKS336 vector (40). The LASV-NP gene that was inserted into the pKS336 vector, pKS336-LASV-NP, was confirmed to be in the correct orientation to the promoter, tested for nucleotide sequencing as described above, and the nucleotide sequence of the gene was confirmed to be identical to the original sequence. HeLa cells were then transfected with pKS336-LASV-NP by using a FuGENE6 transfection reagent (Roche Diagnostics) according to the manufacturer's instructions. The cells transfected with the plasmid were selected with 3 μg of blasticidin *S*-hydrochloride/ml in MEM-10FBS. The HeLa cell clones were analyzed for the expression of LASV-rNP by IIFA using the rabbit serum raised against His-LASV-rNP. The cells expressing LASV-rNP were subcloned and used as IIFA antigens.

Ag-capture ELISA. Ag-capture ELISA was performed as previously described (32, 41). The purified MAb to His-LASV-rNP, MAb 4A5, produced in the present study was diluted in PBS solution, and 100 μl was adsorbed overnight at 4°C onto the immunoplates (96-well type plate, Pro-Bind, Falcon; Becton Dickinson Labware). Purified MAb 4A5 was coated onto the immunoplates at a concentration of approximately 100 ng/well in 100 μl of PBS. The difference in the procedures between the Ag-capture ELISA in the present study and those in

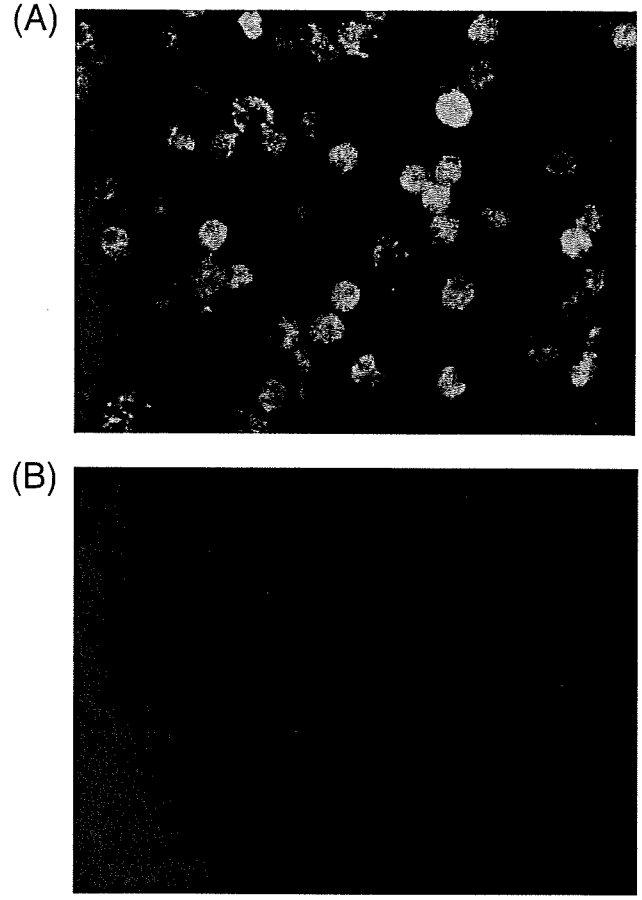

FIG. 3. Staining patterns of LASV-rNP-expressing HeLa cells by sera from an LF patient (A) and a healthy control (B) in an IIFA.

previous studies (32, 37, 41) is that the MAb, MAb 4A5, and rabbit serum raised to His-LASV-rNP were used as capture and detector antibodies, respectively. The procedure for the Ag-capture ELISA was performed as follows. The ELISA plate was coated with capture MAb, followed by blocking of the plate with M-T-PBS, addition of the samples to the ELISA plate, detection of the captured LASV-NP with rabbit serum raised to His-LASV-rNP, detection of rabbit IgG antibody that reacted with the captured antigen with goat anti-rabbit IgG antibodies conjugated with HRPO (Zymed Laboratories), and substrate reaction. In each run of the Ag-capture ELISA, the negative control antigen (M-T-PBS) was also tested. Serially diluted samples were added to the MAb-coated wells. The OD_{405} values of each well were adjusted by subtracting the OD_{405} value of the negative control antigen from the corresponding well. The adjusted OD_{405} was taken as a measure of the amount of antigen specifically bound. All samples were treated with 1% Nonidet-P40 (NP-40) in PBS to destroy the LASV virion and expose the nucleoprotein in the LASV virion.

RT-PCR. RT-PCR was performed as previously described (10). The primers used in the RT-PCR were 36E2 (5'-ACCGGGGATCCTAGGCATT-3') and 80F2 (5'-ATATAATGATGACTGTTGTTCTTTGTGCA-3'). The RT-PCR was carried out with a Ready-to-Go RT-PCR tube (Pharmacia). The amplified PCR products were visualized with ethidium bromide in 2% agarose gel after electrophoresis.

RESULTS

Expression of His-LASV-rNP. Tn*5* cells infected with each of the recombinant baculoviruses—Ac-His-LASV-NP, Ac-LCMV-rNP, and Ac-JUNV-rNP—were suspended in PBS–2 M urea. Most of the cell proteins were solubilized by this

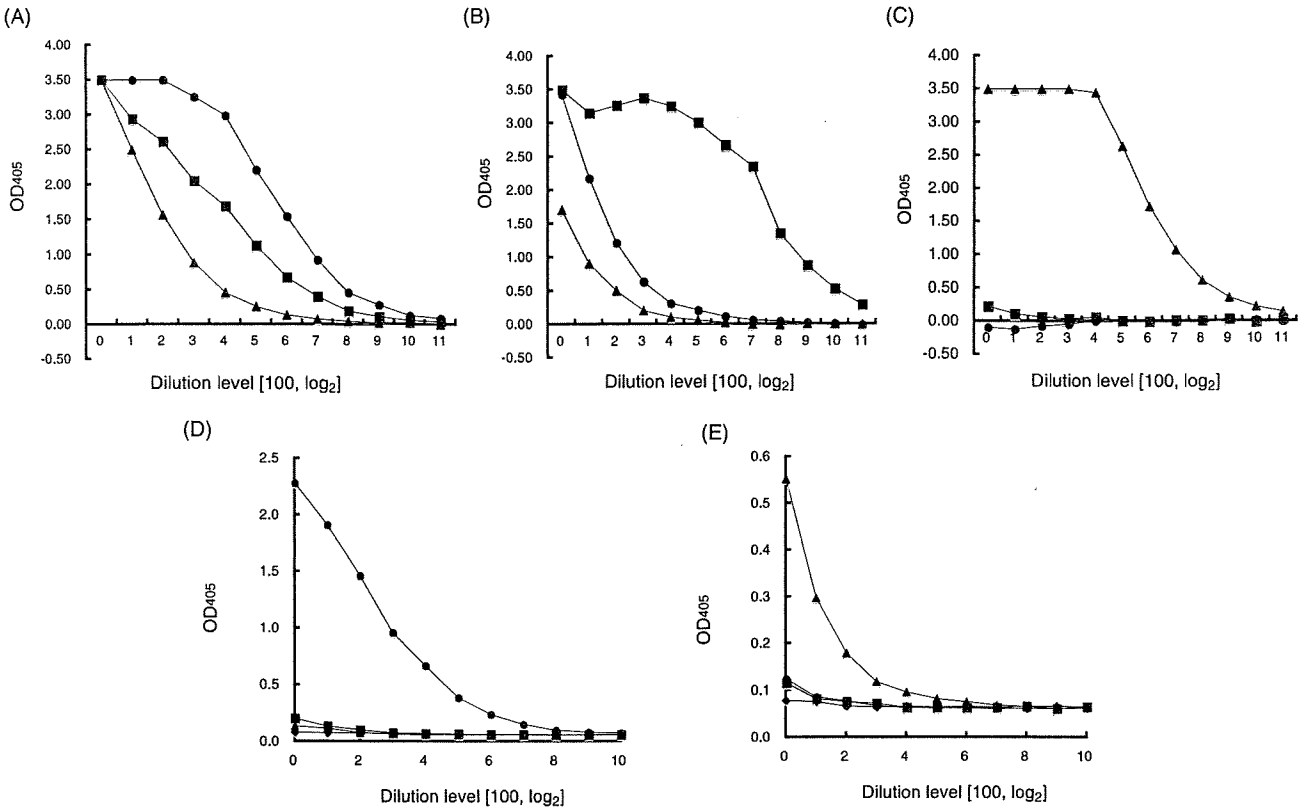

FIG. 4. Reactivity of antibodies to arenaviruses (LASV, LCMV, and JUNV) to the rNPs of these viruses. The reactivities of rabbit sera raised to LASV-rNP (●), LCMV-rNP (■), or JUNV-rNP (▲) with the antigens His-LASV-rNP (A), LCMV-rNP (B), and JUNV-rNP (C) in an IgG-ELISA are shown. The reactivities of the sera collected from patients with LF (D) and AHF (E) with the antigens LASV-rNP (●), LCMV-rNP (▩), and JUNV-rNP (▲) and negative control antigen (◆) in an IgG-ELISA are also shown.

treatment, whereas the rNPs of these viruses remained insoluble. After centrifugation at 15,000 × *g* for 10 min, pellet fractions were collected. The rNPs, which were still present in the pellet fractions, were completely solubilized in PBS–8 M urea. The samples were then centrifuged at 15,000 × *g* for 10 min, and the supernatant fractions of the PBS–8 M urea were confirmed to contain highly purified recombinant rNPs of arenaviruses (Fig. 2).

Development of indirect immunofluorescence. The LASV-rNP was expressed in HeLa cells by transfection with the expression vector, pKS336-LASV-NP. The transfected cells were stained by anti-His-LASV-rNP rabbit serum and human serum samples from LF patients (Fig. 3). All 4 serum samples collected from two LF patients showed a positive staining, but 96 control serum samples did not. The LASV-rNP-based IIFA was also evaluated using serum samples collected from monkeys experimentally infected with LASV. All of the sera collected from five LASV-infected monkeys showed a positive staining, but those from four mock-infected monkeys did not.

Development of His-LASV-rNP-based IgG-ELISA. Four serum samples collected from LF patients were determined to be positive by His-LASV-rNP-based IgG-ELISA, whereas 94 of the 96 control serum samples were determined to be negative. Thus, the sensitivity and specificity of the ELISA were 100 and 96%, respectively. All serum samples collected from five LASV-infected monkeys were determined to be positive, whereas those from four mock-infected monkeys were negative.

In order to examine cross-reactivity among arenaviruses in the LASV-rNP-based IgG-ELISA, antisera against LASV-rNP, LCMV-rNP, or JUNV-rNP were examined (Fig. 4). The anti-LASV-rNP serum showed a strongly positive reaction, and anti-LCMV rNP and anti-JUNV-rNP sera showed strongly positive reactions in the IgG ELISA using the respective antigens (Fig. 4A, B, and C). Anti-LCMV-rNP and anti-JUNV-rNP sera showed a less strongly positive reaction in the His-LASV-rNP-based IgG-ELISA than anti-LASV-rNP serum (Fig. 4A). Anti-LASV-rNP and anti-JUNV-rNP also showed a less strongly positive reaction in the His-LCMV-rNP-based IgG-ELISA than anti-LCMV-rNP serum (Fig. 4B). However, anti-LASV-rNP and anti-LCMV-rNP sera showed a negative reaction in the JUNV-rNP-based IgG-ELISA (Fig. 4C). Human sera from LF patients showed a highly positive reaction in the LASV-rNP-based IgG-ELISA, but sera from patients with Argentine hemorrhagic fever (AHF), which is caused by JUNV, did not (Fig. 4D). Serum from an AHF patient showed a highly positive reaction in the JUNV-rNP-based IgG-ELISA (Fig. 4E). These results suggest that cross-reactive antibody among arenaviruses may be detected by the newly developed LASV-rNP-based IgG-ELISA.

Development of LASV Ag-capture ELISA. Three clones of a hybridoma that excreted an MAb to His-LASV-rNP were es-

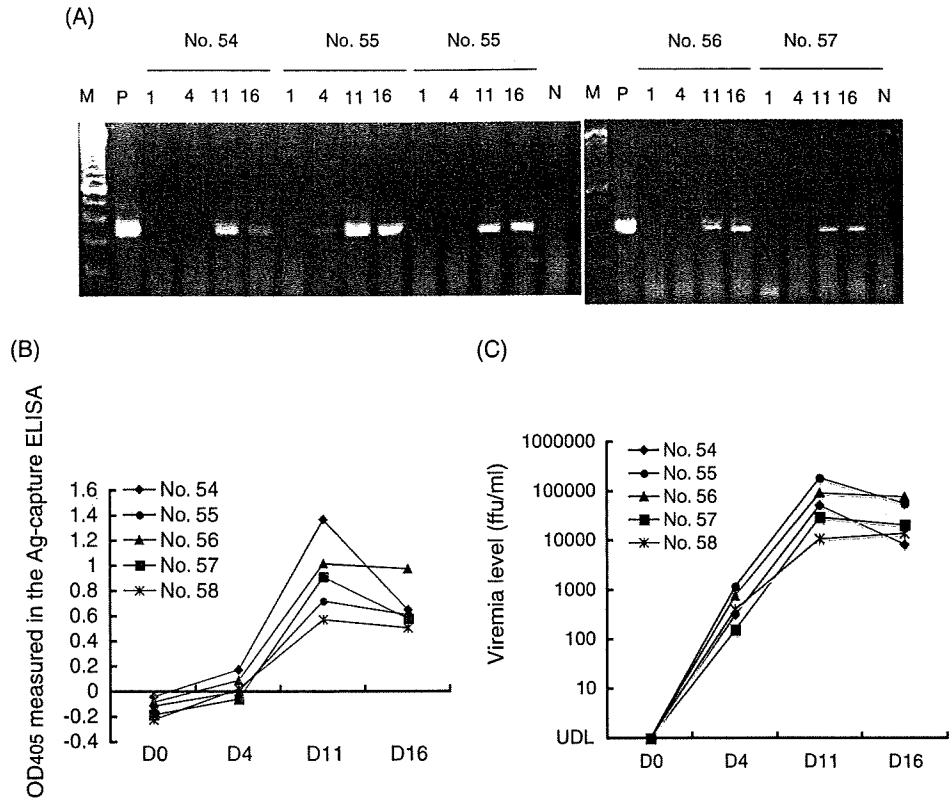

FIG. 5. Detection of the LASV genome by the RT-PCR (A), LASV-NP by the LASV-NP-Ag-capture ELISA (B), and the infectious dose of LASV (C) in serially collected sera of hamsters experimentally infected with LASV. The OD_{405} values in panel B were obtained at a dilution of 1:40.

tablished. The isotype of the three MAbs were identified as IgG1. These MAbs were designated MAb 4A5, MAb 6C11, and MAb 2-11. Of these MAbs, MAb 4A5 was the most efficient in capturing His-LASV-rNP in the Ag-capture ELISA format. The Ag-capture ELISA with MAb 4A5 detected His-LASV-rNP concentrations as low as 800 pg/ml (data not shown). Furthermore, the Ag-capture ELISA detected the MOPV-NP but not the rNPs of LCMV and JUNV (data not shown).

All of the sera collected from five LASV-infected hamsters on days 11 and 16 postinfection were antigen positive in the Ag-capture ELISA using MAb 4A5 as a capture antibody, whereas the sera collected on days 0 and 4 were antigen negative. The OD_{405} values in the ELISA were highest on day 11. The reactivity patterns in each hamster in the ELISA were similar to the viremia levels (Fig. 5). The sera collected on days 11 and 16 were found to be LASV genome positive by RT-PCR (10). Thus, the sensitivity of the Ag-capture ELISA was similar to that of the RT-PCR.

Determination of the epitope recognized by the monoclonal antibodies. The epitope recognized by MAbs was determined. MAb-4A5 reacted in Western blots with GST-LASV-rNP1-6 (full-length LASV-rNP), GST-LASV-rNP1-5, and GST-LASV-rNP1-4 but not with the other truncated LASV-rNPs shown in Table 1, suggesting that MAb 4A5 reacted with a conformational epitope located on the amino-terminal portion of LASV-rNP. The epitope was maintained when the extreme amino-terminal portion, LASV-rNP1, was present but was lost when LASV-rNP1 was removed. These results suggest that the extreme amino-terminal portion, LASV-rNP1, is essential for the maintenance of the conformational epitope. MAbs 6C11 and 2-11 reacted in Western blots with GST-LASV-rNP1 and GST-LASV-rNP5, respectively (Table 1).

The Pepscan analyses indicated that MAbs 6C11 and 2-11

TABLE 1. Reactivities of the MAbs developed in the present study with the GST-tagged truncated LASV-rNP in Western blot analyses

Truncated LASV-rNP	Reactivity with MAb[a]:		
	6C11	4A5	2-11
LASV-rNP1	+	–	–
LASV-rNP2	–	–	–
LASV-rNP3	–	–	–
LASV-rNP4	–	–	–
LASV-rNP5	–	–	+
LASV-rNP6	–	–	–
LASV-rNP1-2	ND	–	ND
LASV-rNP1-3	ND	–	ND
LASV-rNP1-4	ND	+	ND
LASV-rNP1-5	ND	+	ND
LASV-rNP1-6[b]	ND	+	ND
LASV-rNP2-7	ND	–	ND
LASV-rNP3-6	ND	–	ND
LASV-rNP4-6	ND	–	ND
LASV-rNP5-6	ND	–	ND

[a] "+" and "–" indicate positive and negative reactions, respectively. ND, not determined.
[b] LASV-rNP1-6 indicates LASV-rNP.

TABLE 2. Reactivities of the MAbs developed in the present study with the NPs of LASV, MOPV, LCMV, and JUNV in Western blot analyses

MAb	Reactivity of MAb[a] with NP of:			
	LASV	MOPV	LCMV	JUNV
4A5	+	+	–	–
6C11	+	ND	+	–
2-11	+	ND	–	–

[a] "+" and "–" indicate positive and negative reactions, respectively. ND, not determined. The reactivities of MAb 6C11 and MAb 2-11 were not evaluated with MOPV-NP. However, theoretically, MAb 6C11 should be reactive with MOPV-NP due to the presence of the amino acid residues that can react with MAb 6C11, but MAb 2-11 should not react with MOPV-NP due to the absence of the amino acid residues that can react with MAb 2-11.

recognized linear epitopes. MAbs 6C-11 and 2-11 recognized GLDFSEV (aa 41 to 47) within LASV-rNP1 and FATQP (aa 439 to 443) within LASV-rNP5, respectively (Fig. 6). The reactivity patterns of these MAbs with NPs of LASV, MOPV, LCMV, and JUNV are summarized in Table 2.

DISCUSSION

We report here the development of diagnostic systems (antibody and antigen detection systems) for LF using LASV-rNP. The LASV-rNP-based IgG-ELISA was sensitive and specific in detecting anti-LASV-IgG. Although the data were not shown, an IgM-capture ELISA using purified LASV-rNP as an antigen was developed in the same way as that shown in previous reports and detected LASV-IgM antibody (42, 43). All sera collected from LF patients and monkeys infected with LASV showed positive reactions in the LASV-rNP-based IIFA. The staining patterns of the rNP with these sera were granular in the IIFA (Fig. 3), making it easy to distinguish positives from negatives. IIFA using LASV-rNP-expressing HeLa cells was also highly sensitive and specific in detecting LASV-IgG. In the preliminary study, ca. 15% of the sera collected from 334 Ghanaians and only less than 1% of 280 Zambians showed positive reactions in the LASV-rNP-based IgG ELISA (our data). The results are considered to be compatible with the fact that LF is endemic to the western African region, including Ghana, but not to the eastern African region. The LASV-rNP-based antibody detection systems such as ELISA and IIFA were suggested to be useful not only in the diagnosis of but also in the seroepidemiological study of LF.

The LASV-rNPs were expressed by a transformation system in *E. coli* or by recombinant baculovirus systems and have already been applied as antigens in ELISA, Western blotting, and IIFA for the detection of antibodies to LASV (4, 14, 16, 22, 23, 44). In the present study, an Ag-capture ELISA using

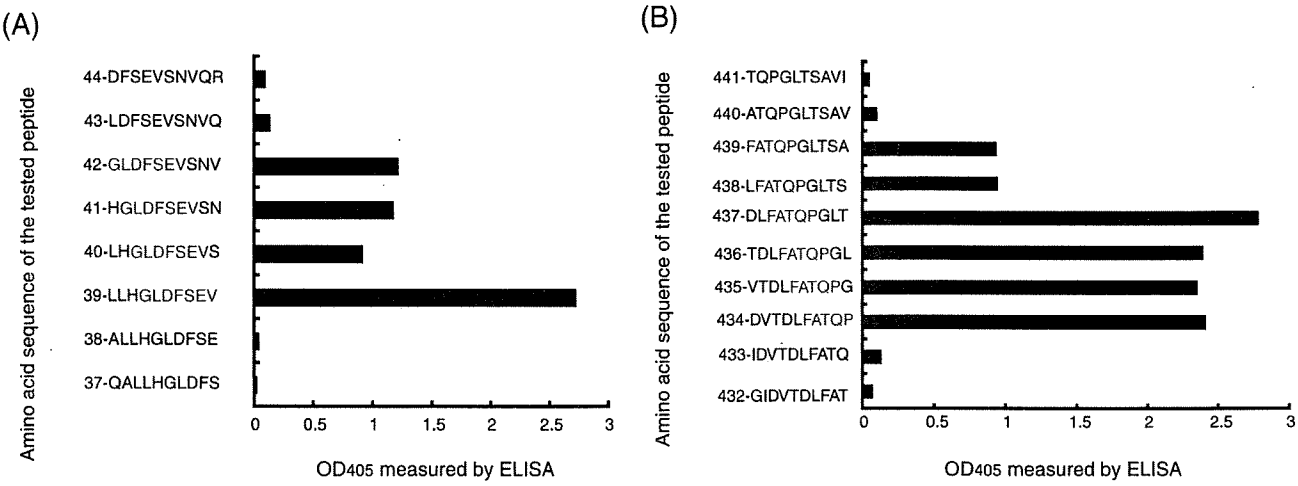

(C)

Arenavirus-NP	Amino acid sequence of the corresponding region: MoAb-6C11	MoAb-2-11
LASV-NP	31-VVKDAQALLHGLDFSEVNVQRLMRKERRD	431-HGIDVTDLFATQPGLTSAVI
MOPV-NP	31-VIKDAQALLHGLDFSEVANVQRLMRKEKRD	432-HGIDIQDLFSVQPGLTSAVI
LCMV-NP	31-VIKDATNLLNGLDFSEVSNVQRIMRKEKRD	424-HGMDLADLFNAQPGLTSSVI
JUNV-NP	31-VLKDAKLIADSIDFNQVAQVQRALRKTKRG	422-HGILMKDIEDAMPGVLSYVI

FIG. 6. Pepscan analyses to determine the epitopes of MAb 6C11 (A) and MAb 2-11 (B). The vertical bar indicates the amino acid residues with an amino acid position within the LASV-NP. MAb 6C11 was confirmed to react with 7 aa residues positioned from aa 42 to 48 (GLDFSEV) within LASV-NP1. MoAb-2-11 was confirmed to react with 5 aa residues positioned from aa 439 to 443 (FATQP) within LASV-NP5. (C) The corresponding amino acid residues to the epitope of the MAb 6C11 and MAb 2-11 among MOPV, LCMV, and JUNV are shown. The GenBank accession numbers for the S genes of LASV, MOPV, LCMV, and JUNV are NC_004296, AY772170, AY847350, and DQ272266, respectively. The epitope of the MAb 6C11 is present not only in the nucleoprotein of LASV but also in those of MOPV and LCMV—but not in that of JUNV.

MAbs to LASV-rNP was also developed. Furthermore, detection of the cross-reactive antibody by LASV-rNP-based IgG-ELISA was examined. The results for cross-reactivity indicate that the LASV-rNP-based IgG-ELISA detects not only antibodies to LASV but also those to LCMV.

The Ag-capture ELISA using MAb 4A5 was confirmed to be useful in the detection of authentic LASV antigen in sera serially collected from hamsters infected with LASV. The sensitivity of the MAb 4A5-based Ag-ELISA was similar to that of conventional RT-PCR, the efficiency of which in the diagnosis of LF was previously reported (10). Therefore, the MAb 4A5-based Ag-capture ELISA is regarded as useful in the diagnosis of LF. Unfortunately, the efficacy of the MAb 4A5-based Ag-capture ELISA in the diagnosis of LF was not evaluated using serum samples from patients. Thus, further study is still required. The three MAbs, including MAb 4A5, were characterized, and the corresponding amino acid residues within the nucleoproteins of LASV, MOPV, LCMV, and JUNV to the epitopes of MAb 6C11 and MAb 2-11 are summarized in Fig. 6C. It was of interest that LASV, MOPV, LCMV, and JUNV might be identified by analyses of the reactivity patterns of MAbs 4A5, 6C11, and 2-11 to the nucleoproteins of each virus. The nucleoproteins of all LASV strains circulating in the western and central parts of Africa would be detected by the MAb 4A5-based Ag-capture ELISA, since this ELISA was able to detect MOPV-NP that was different from LASV in terms of genetic and evolutional characteristics.

We have thus far reported the development of antibody and antigen detection systems using the recombinant nucleoproteins of the viruses for Ebola hemorrhagic fever, Marburg hemorrhagic fever, and Crimean-Congo hemorrhagic fever (32, 33, 36–42). Recently, a number of highly pathogenic emerging virus infections in humans appeared, such as Nipah virus encephalitis (8), SARS-coronavirus infections (21, 35), and highly pathogenic avian influenza virus infections (9, 45, 46). The strategy shown here might be applicable to the development of diagnostic systems for severe viral infections whose etiologic agents are highly pathogenic to humans as an alternative method to methods using infectious viruses.

ACKNOWLEDGMENTS

We thank M. Ogata, Department of Virology 1, National Institute of Infectious Diseases, Tokyo, Japan, for great clerical assistance.

This study was partly supported by a grant-in-aid for scientific research from the Ministry of Health, Labor, and Welfare of Japan; by the Japan Health Sciences Foundation (grant 16171301); and by the Japan Society for Promotion of Science (grant 18591210).

REFERENCES

1. **Anonymous.** 2000. Lassa fever imported to England. Commun. Dis. Rep. CDR Wkly. **10**:99.
2. **Anonymous.** 2000. Lassa fever, imported case, The Netherlands. Wkly. Epidemiol. Rec. **75**:265.
3. **Baize, S., D. Pannetier, C. Faure, P. Marianneau, I. Marendat, M. C. Georges-Courbot, and V. Deubel.** 2006. Role of interferons in the control of Lassa virus replication in human dendritic cells and macrophages. Microbes Infect. **8**:1194–1202.
4. **Barber, G. N., J. C. Clegg, and G. Lloyd.** 1990. Expression of the Lassa virus nucleocapsid protein in insect cells infected with a recombinant baculovirus: application to diagnostic assays for Lassa virus infection. J. Gen. Virol. **71**(Pt. 1):19–28.
5. **Borio, L., T. Inglesby, C. J. Peters, A. L. Schmaljohn, J. M. Hughes, P. B. Jahrling, T. Ksiazek, K. M. Johnson, A. Meyerhoff, T. O'Toole, M. S. Ascher, J. Bartlett, J. G. Breman, E. M. Eitzen, Jr., M. Hamburg, J. Hauer, D. A. Henderson, R. T. Johnson, G. Kwik, M. Layton, S. Lillibridge, G. J. Nabel, M. T. Osterholm, T. M. Perl, P. Russell, and K. Tonat.** 2002. Hemorrhagic fever viruses as biological weapons: medical and public health management. JAMA **287**:2391–2405.
6. **Bossi, P., A. Tegnell, A. Baka, F. Van Loock, J. Hendriks, A. Werner, H. Maidhof, and G. Gouvras.** 2004. Bichat guidelines for the clinical management of haemorrhagic fever viruses and bioterrorism-related haemorrhagic fever viruses. Eur. Surveill. **9**:E11–E12.
7. **Carey, D. E., G. E. Kemp, H. A. White, L. Pinneo, R. F. Addy, A. L. Fom, G. Stroh, J. Casals, and B. E. Henderson.** 1972. Lassa fever. Epidemiological aspects of the 1970 epidemic, Jos, Nigeria. Trans. R. Soc. Trop. Med. Hyg. **66**:402–408.
8. **Chua, K. B., K. J. Goh, K. T. Wong, A. Kamarulzaman, P. S. Tan, T. G. Ksiazek, S. R. Zaki, G. Paul, S. K. Lam, and C. T. Tan.** 1999. Fatal encephalitis due to Nipah virus among pig-farmers in Malaysia. Lancet **354**:1257–1259.
9. **Claas, E. C., A. D. Osterhaus, R. van Beek, J. C. De Jong, G. F. Rimmelzwaan, D. A. Senne, S. Krauss, K. F. Shortridge, and R. G. Webster.** 1998. Human influenza A H5N1 virus related to a highly pathogenic avian influenza virus. Lancet **351**:472–477.
10. **Demby, A. H., J. Chamberlain, D. W. Brown, and C. S. Clegg.** 1994. Early diagnosis of Lassa fever by reverse transcription-PCR. J. Clin. Microbiol. **32**:2898–2903.
11. **Ghiringhelli, P. D., R. V. Rivera Pomar, N. I. Baro, M. F. Rosas, O. Grau, and V. Romanowski.** 1989. Nucleocapsid protein gene of Junin arenavirus (cDNA sequence). Nucleic Acids Res. **17**:8001.
12. **Ghiringhelli, P. D., R. V. Rivera-Pomar, M. E. Lozano, O. Grau, and V. Romanowski.** 1991. Molecular organization of Junin virus S RNA: complete nucleotide sequence, relationship with other members of the *Arenaviridae* and unusual secondary structures. J. Gen. Virol. **72**(Pt. 9):2129–2141.
13. **Gunther, S., P. Emmerich, T. Laue, O. Kuhle, M. Asper, A. Jung, T. Grewing, J. ter Meulen, and H. Schmitz.** 2000. Imported Lassa fever in Germany: molecular characterization of a new Lassa virus strain. Emerg. Infect. Dis. **6**:466–476.
14. **Gunther, S., O. Kuhle, D. Rehder, G. N. Odaibo, D. O. Olaleye, P. Emmerich, J. ter Meulen, and H. Schmitz.** 2001. Antibodies to Lassa virus Z protein and nucleoprotein co-occur in human sera from Lassa fever endemic regions. Med. Microbiol. Immunol. **189**:225–229.
15. **Hirabayashi, Y., S. Oka, H. Goto, K. Shimada, T. Kurata, S. P. Fisher-Hoch, and J. B. McCormick.** 1988. An imported case of Lassa fever with late appearance of polyserositis. J. Infect. Dis. **158**:872–875.
16. **Hummel, K. B., M. L. Martin, and D. D. Auperin.** 1992. Baculovirus expression of the glycoprotein gene of Lassa virus and characterization of the recombinant protein. Virus Res. **25**:79–90.
17. **Ikegami, T., M. Niikura, M. Saijo, M. E. Miranda, A. B. Calaor, M. Hernandez, L. P. Acosta, D. L. Manalo, I. Kurane, Y. Yoshikawa, and S. Morikawa.** 2003. Antigen capture enzyme-linked immunosorbent assay for specific detection of Reston Ebola virus nucleoprotein. Clin. Diagn. Lab. Immunol. **10**:552–557.
18. **Jeffs, B.** 2006. A clinical guide to viral haemorrhagic fevers: Ebola, Marburg, and Lassa. Trop. Doct. **36**:1–4.
19. **King, L., and R. Possee.** 1992. The baculovirus expression system: a laboratory guide. Chapman and Hall, New York, NY.
20. **Kitts, P. A., M. D. Ayres, and R. D. Possee.** 1990. Linearization of baculovirus DNA enhances the recovery of recombinant virus expression vectors. Nucleic Acids Res. **18**:5667–5672.
21. **Ksiazek, T. G., D. Erdman, C. S. Goldsmith, S. R. Zaki, T. Peret, S. Emery, S. Tong, C. Urbani, J. A. Comer, W. Lim, P. E. Rollin, S. F. Dowell, A. E. Ling, C. D. Humphrey, W. J. Shieh, J. Guarner, C. D. Paddock, P. Rota, B. Fields, J. DeRisi, J. Y. Yang, N. Cox, J. M. Hughes, J. W. LeDuc, W. J. Bellini, and L. J. Anderson.** 2003. A novel coronavirus associated with severe acute respiratory syndrome. N. Engl. J. Med. **348**:1953–1966.
22. **Lloyd, G., G. N. Barber, J. C. Clegg, and P. Kelly.** 1989. Identification of Lassa fever virus infection with recombinant nucleocapsid protein antigen. Lancet **ii**:1222.
23. **Lukashevich, L. S., J. C. Clegg, and K. Sidibe.** 1993. Lassa virus activity in Guinea: distribution of human antiviral antibody defined using enzyme-linked immunosorbent assay with recombinant antigen. J. Med. Virol. **40**: 210–217.
24. **Macher, A. M., and M. S. Wolfe.** 2006. Historical Lassa fever reports and 30-year clinical update. Emerg. Infect. Dis. **12**:835–837.
25. **Mahdy, M. S., W. Chiang, B. McLaughlin, K. Derksen, B. H. Truxton, and K. Neg.** 1989. Lassa fever: the first confirmed case imported into Canada. Can. Dis. Wkly. Rep. **15**:193–198.
26. **Matsuura, Y., R. D. Possee, and D. H. Bishop.** 1986. Expression of the S-coded genes of lymphocytic choriomeningitis arenavirus using a baculovirus vector. J. Gen. Virol. **67**(Pt. 8):1515–1529.
27. **McCormick, J. B., P. A. Webb, J. W. Krebs, K. M. Johnson, and E. S. Smith.** 1987. A prospective study of the epidemiology and ecology of Lassa fever. J. Infect. Dis. **155**:437–444.
28. **Merryweather, A. T., U. Weyer, M. P. Harris, M. Hirst, T. Booth, and R. D. Possee.** 1990. Construction of genetically engineered baculovirus insecticides

containing the *Bacillus thuringiensis* subsp. *kurstaki* HD-73 delta endotoxin. J. Gen. Virol. **71**(Pt. 7):1535–1544.
29. **Monath, T. P.** 1975. Lassa fever: review of epidemiology and epizootiology. Bull. W. H. O. **52**:577–592.
30. **Monath, T. P., P. E. Mertens, R. Patton, C. R. Moser, J. J. Baum, L. Pinneo, G. W. Gary, and R. E. Kissling.** 1973. A hospital epidemic of Lassa fever in Zorzor, Liberia, March-April 1972. Am. J. Trop. Med. Hyg. **22**:773–779.
31. **Monson, M. H., J. D. Frame, P. B. Jahrling, and K. Alexander.** 1984. Endemic Lassa fever in Liberia. I. Clinical and epidemiological aspects at Curran Lutheran Hospital, Zorzor, Liberia. Trans. R. Soc. Trop. Med. Hyg. **78**:549–553.
32. **Niikura, M., T. Ikegami, M. Saijo, I. Kurane, M. E. Miranda, and S. Morikawa.** 2001. Detection of Ebola viral antigen by enzyme-linked immunosorbent assay using a novel monoclonal antibody to nucleoprotein. J. Clin. Microbiol. **39**:3267–3271.
33. **Niikura, M., T. Ikegami, M. Saijo, T. Kurata, I. Kurane, and S. Morikawa.** 2003. Analysis of linear B-cell epitopes of the nucleoprotein of Ebola virus that distinguish Ebola virus subtypes. Clin. Diagn. Lab. Immunol. **10**:83–87.
34. **Peters, C. J.** 2002. Clinical virology, p. 949–969. *In* D. D. Richman, R. J. Whitley, and F. G. Hayden (ed.), Arenaviruses, 2nd ed. ASM Press, Washington, DC.
35. **Rota, P. A., M. S. Oberste, S. S. Monroe, W. A. Nix, R. Campagnoli, J. P. Icenogle, S. Penaranda, B. Bankamp, K. Maher, M. H. Chen, S. Tong, A. Tamin, L. Lowe, M. Frace, J. L. DeRisi, Q. Chen, D. Wang, D. D. Erdman, T. C. Peret, C. Burns, T. G. Ksiazek, P. E. Rollin, A. Sanchez, S. Liffick, B. Holloway, J. Limor, K. McCaustland, M. Olsen-Rasmussen, R. Fouchier, S. Gunther, A. D. Osterhaus, C. Drosten, M. A. Pallansch, L. J. Anderson, and W. J. Bellini.** 2003. Characterization of a novel coronavirus associated with severe acute respiratory syndrome. Science **300**:1394–1399.
36. **Saijo, M., M. Niikura, T. Ikegami, I. Kurane, T. Kurata, and S. Morikawa.** 2006. Laboratory diagnostic systems for Ebola and Marburg hemorrhagic fevers developed with recombinant proteins. Clin. Vaccine Immunol. **13**: 444–451.
37. **Saijo, M., M. Niikura, A. Maeda, T. Sata, T. Kurata, I. Kurane, and S. Morikawa.** 2005. Characterization of monoclonal antibodies to Marburg virus nucleoprotein (NP) that can be used for NP-capture enzyme-linked immunosorbent assay. J. Med. Virol. **76**:111–118.
38. **Saijo, M., M. Niikura, S. Morikawa, T. G. Ksiazek, R. F. Meyer, C. J. Peters, and I. Kurane.** 2001. Enzyme-linked immunosorbent assays for detection of antibodies to Ebola and Marburg viruses using recombinant nucleoproteins. J. Clin. Microbiol. **39**:1–7.
39. **Saijo, M., T. Qing, M. Niikura, A. Maeda, T. Ikegami, C. Prehaud, I. Kurane, and S. Morikawa.** 2002. Recombinant nucleoprotein-based enzyme-linked immunosorbent assay for detection of immunoglobulin G antibodies to Crimean-Congo hemorrhagic fever virus. J. Clin. Microbiol. **40**:1587–1591.
40. **Saijo, M., T. Qing, M. Niikura, A. Maeda, T. Ikegami, K. Sakai, C. Prehaud, I. Kurane, and S. Morikawa.** 2002. Immunofluorescence technique using HeLa cells expressing recombinant nucleoprotein for detection of immunoglobulin G antibodies to Crimean-Congo hemorrhagic fever virus. J. Clin. Microbiol. **40**:372–375.
41. **Saijo, M., Q. Tang, B. Shimayi, L. Han, Y. Zhang, M. Asiguma, D. Tianshu, A. Maeda, I. Kurane, and S. Morikawa.** 2005. Antigen-capture enzyme-linked immunosorbent assay for the diagnosis of Crimean-Congo hemorrhagic fever using a novel monoclonal antibody. J. Med. Virol. **77**:83–88.
42. **Saijo, M., Q. Tang, B. Shimayi, L. Han, Y. Zhang, M. Asiguma, D. Tianshu, A. Maeda, I. Kurane, and S. Morikawa.** 2005. Recombinant nucleoprotein-based serological diagnosis of Crimean-Congo hemorrhagic fever virus infections. J. Med. Virol. **75**:295–299.
43. **Tang, Q., M. Saijo, Y. Zhang, M. Asiguma, D. Tianshu, L. Han, B. Shimayi, A. Maeda, I. Kurane, and S. Morikawa.** 2003. A patient with Crimean-Congo hemorrhagic fever serologically diagnosed by recombinant nucleoprotein-based antibody detection systems. Clin. Diagn. Lab. Immunol. **10**:489–491.
44. **Ter Meulen, J., K. Koulemou, T. Wittekindt, K. Windisch, S. Strigl, S. Conde, and H. Schmitz.** 1998. Detection of Lassa virus antinucleoprotein immunoglobulin G (IgG) and IgM antibodies by a simple recombinant immunoblot assay for field use. J. Clin. Microbiol. **36**:3143–3148.
45. **Tran, T. H., T. L. Nguyen, T. D. Nguyen, T. S. Luong, P. M. Pham, V. C. Nguyen, T. S. Pham, C. D. Vo, T. Q. Le, T. T. Ngo, B. K. Dao, P. P. Le, T. T. Nguyen, T. L. Hoang, V. T. Cao, T. G. Le, D. T. Nguyen, H. N. Le, K. T. Nguyen, H. S. Le, V. T. Le, D. Christiane, T. T. Tran, J. Menno de, C. Schultsz, P. Cheng, W. Lim, P. Horby, and J. Farrar.** 2004. Avian influenza A (H5N1) in 10 patients in Vietnam. N. Engl. J. Med. **350**:1179–1188.
46. **Yuen, K. Y., P. K. Chan, M. Peiris, D. N. Tsang, T. L. Que, K. F. Shortridge, P. T. Cheung, W. K. To, E. T. Ho, R. Sung, and A. F. Cheng.** 1998. Clinical features and rapid viral diagnosis of human disease associated with avian influenza A H5N1 virus. Lancet **351**:467–471.

Available online at www.sciencedirect.com
ScienceDirect
Virus Research 123 (2007) 120–127
Virus Research
www.elsevier.com/locate/virusres

Increased permeability of human endothelial cell line EA.hy926 induced by hantavirus-specific cytotoxic T lymphocytes

Daisuke Hayasaka, Ken Maeda [1], Francis A. Ennis, Masanori Terajima*

Center for Infectious Disease and Vaccine Research, University of Massachusetts Medical School, 55 Lake Avenue North, Worcester, MA 01655, USA

Received 19 April 2006; received in revised form 14 August 2006; accepted 16 August 2006
Available online 18 September 2006

Abstract

Hantavirus infection causes two human diseases, hemorrhagic fever with renal syndrome and hantavirus pulmonary syndrome. The typical feature of these diseases is increased permeability in microvascular beds in the kidneys and the lungs, respectively. The mechanism of capillary leakage, however, is not understood. Some evidence suggests that hantavirus disease pathogenesis is immunologically mediated by cytotoxic T lymphocytes and other immune cells in target organs producing inflammatory cytokines. In this study we examined the roles of virus-specific cytotoxic T lymphocytes in increased permeability of human endothelial cells infected with hantavirus. We used a human $CD8^+$ hantavirus-specific cytotoxic T lymphocyte line, 1A-E2, specific for the HLA-A24-restricted epitope in Sin Nombre and Puumala virus G2 protein, and the human endothelial cell line, EA.hy926 that expresses HLA-A24 molecule. The cytotoxic T lymphocyte line recognized and lysed target cells infected with Sin Nombre virus, and in transwell permeability assays increased permeability of EA.hy926 cell monolayer infected with Sin Nombre virus or recombinant adenovirus expressing the Sin Nombre virus G2 protein. These results suggest that cytotoxic T lymphocyte activity contribute to capillary leakage observed in patients with hantavirus pulmonary syndrome or hemorrhagic fever with renal syndrome.
Published by Elsevier B.V.

Keywords: Sin Nombre virus; Hantavirus pulmonary syndrome; Hemorrhagic fever with renal syndrome; Cytotoxic T lymphocyte; Endothelial cell; Transwell permeability assay

1. Introduction

Hantaviruses, belonging to the family Bunyaviridae, are distributed worldwide. Two forms of zoonotic human diseases are caused by hantavirus species (Enria et al., 2001; Linderholm and Elgh, 2001; Schmaljohn and Hjelle, 1997). Hemorrhagic fever with renal syndrome (HFRS) and its mild form nephropathia epidemica (NE) are caused by Old World (Europe and Asia) hantaviruses, such as Hantaan, Seoul, Dobrava and Puumala viruses. Hantavirus pulmonary syndrome (HPS) is caused by New World (North and South America) hantaviruses, such as Sin Nombre and Andes viruses (Khaiboullina and St Jeor, 2002; Zeier et al., 2005). The hantavirus genome consists of three RNA segments, large, medium and small segments, encoding RNA-dependent RNA polymerase, envelope glycoproteins (G1 and G2), and nucleocapsid (N) protein, respectively (Jonsson and Schmaljohn, 2001). Hantaviruses persistently infect their natural rodent reservoirs without apparent diseases (Meyer and Schmaljohn, 2000). Humans are infected with hantaviruses by direct contact with infected rodents or through the inhalation of excreted viral aerosols (Linderholm and Elgh, 2001).

Human hantavirus diseases are characterized by an increased permeability in microvascular beds of the kidneys in HFRS and the lungs in HPS, and endothelial cells are considered to be the primary targets of hantavirus infection (Hautala et al., 2002; Khaiboullina and St Jeor, 2002; Mustonen et al., 1994; Temonen et al., 1996; Zaki et al., 1995). In vitro hantavirus infection alone, however, did not induce visible cytopathic effects in cultured human endothelial cells (Geimonen et al., 2002; Niikura et al., 2004; Pensiero et al., 1992) nor did it increase capillary permeability of an infected endothelial cell monolayer (Khaiboullina et al., 2000; Niikura et al., 2004; Sundstrom et al., 2001). Increased levels of cytokines including

* Corresponding author. Tel.: +1 508 856 6854; fax: +1 508 856 4890.
E-mail addresses: Daisuke.Hayasaka@umassmed.edu (D. Hayasaka), kmaeda@yamaguchi-u.ac.jp (K. Maeda), Francis.Ennis@umassmed.edu (F.A. Ennis), Masanori.Terajima@umassmed.edu (M. Terajima).
[1] Present address: Department of Veterinary Microbiology, Faculty of Agriculture, Yamaguchi University, 1677-1 Yoshida, Yamaguchi 753-8515, Japan.

0168-1702/$ – see front matter. Published by Elsevier B.V.
doi:10.1016/j.virusres.2006.08.006

tumor necrosis factor (TNF) -α, interleukin (IL) -2, IL-6 and interferon (IFN) -γ have been detected in sera of HFRS and HPS patients (Khaiboullina and St Jeor, 2002; Vapalahti et al., 2001). An expanded leukocyte population including monocytes, T and B cells and an increase of $CD8^+/CD4^+$ ratio have been observed in HFRS patients (Chen and Yang, 1990; Huang et al., 1994; Lewis et al., 1991; Markotic et al., 1999). We found significantly higher frequencies of Sin Nombre virus (SNV)-specific T cells in patients with severe HPS requiring mechanical ventilation (up to 44.2% of $CD8^+$ T cells) than in moderately ill HPS patients hospitalized but not requiring mechanical ventilation (up to 9.8% of $CD8^+$ T cells). These results suggest that virus-specific $CD8^+$ T cells contribute to HPS disease outcome (Kilpatrick et al., 2004). Increased numbers of $CD8^+$ T cells are found in the kidneys of HFRS (Temonen et al., 1996) and in the lungs of HPS patients (Zaki et al., 1995). There is an abundance of immune cells expressing a variety of cytokines in the lungs of HPS cases (Mori et al., 1999; Zaki et al., 1995) and in the kidneys of NE cases (Temonen et al., 1996). In addition, preliminary evidence suggests that HLA-B*3501 is associated with severe HPS in SNV infection, implying involvement of $CD8^+$ cytotoxic T lymphocytes (CTLs) (Kilpatrick et al., 2004) (Koster et al., 2001). A similar linkage between disease severity and MHC haplotype was observed between Puumala virus infection and the HLA-B8-DR3 extended haplotype (severe outcome) or the HLA-B27 (milder disease) (Makela et al., 2002; Mustonen et al., 1998). These reports suggest that host immune responses against hantavirus, especially virus-specific CTLs and inflammatory cytokines produced by virus-specific T cells may contribute to disease pathogenesis of HPS and HFRS (Terajima et al., 2004).

We have established panels of CTL lines from the PBMC of NE and HPS patients (Ennis et al., 1997; Kilpatrick et al., 2004; Terajima et al., 2002, 2004; Van Epps et al., 1999, 2002). These cell lines were able to recognize and lyse autologous B lymphoblastoid cell lines pulsed with the epitope peptide or infected with recombinant vaccinia viruses expressing the hantaviral protein containing the epitope. In this report, we tested one of these CTL lines against human endothelial cell line, EA.hy926, infected with SNV in vitro. Primary human umbilical vein endothelial cells (HUVECs) or human lung microvascular endothelial cells (HMVEC-Ls) have been used to examine the effect of hantavirus infection on endothelial cell function (Gavrilovskaya et al., 2002; Khaiboullina et al., 2000; Niikura et al., 2004; Sundstrom et al., 2001). Although ideally the interaction between hantavirus-specific CTL and hantavirus-infected endothelial cells should also be analyzed using HUVECs or HMVEC-Ls, it is difficult to obtain endothelial cells that express the MHC class I molecules by which our CTL lines were restricted. Therefore, we used the immortalized human endothelial cell line EA.hy926 (Edgell et al., 1983), which we found to express the HLA-A24 allele (in this report), and one of our hantavirus-specific CTL line, 1A-E2, which was established from convalescent PBMC from the patient infected with Puumala virus and was restricted by HLA-A24 (Terajima et al., 2002). 1A-E2 recognized the epitope, HWMDATFNL, encoded by Puumala virus G2 protein, and was cross-reactive to the corresponding peptide, HWMDGTFNI, in SNV G2 protein (Terajima et al., 2002). EA.hy926 cells are the most similar to HUVEC among the available immortalized human endothelial cell lines and have been used to study the endothelial cell/leukocyte interactions (Lidington et al., 1999).

In this study, we first tested the infectivity of SNV to EA.hy926 cells. Next, we showed that the hantavirus-specific $CD8^+$ T cell line 1A-E2 could recognize and lyse EA.hy926 cells infected with SNV or presenting SNV antigen. Finally, we demonstrated that 1A-E2 enhanced the permeability of EA.hy926 cells infected with SNV. These results suggest that virus-specific CTLs contribute to the capillary leakage.

2. Materials and methods

2.1. Virus and cell lines

SNV stock virus (strain CC107, kindly provided by Connie S. Schmaljohn) (Schmaljohn et al., 1995) was propagated in Vero E6 cells and aliquots were stored in −80 °C. All experiments using cultured live SNV were performed in biosafety level 3 laboratory of University of Massachusetts Medical School according to standard BSL3 guidelines. The EA.hy926 cell line, which had been derived by fusing HUVECs with the permanent human cell line A549, were kindly provided by Cora-Jean S. Edgell, University of North Carolina (Edgell et al., 1983). Vero E6 cells (ATCC CRL-1586) and EA.hy926 cells were maintained in Dulbecco's modified Eagle's medium (DMEM) (Invitrogen Corporation, Carlsbad, CA) containing 2% fetal bovine serum (FBS). CTL line, 1A-E2, was established from convalescent PBMC of the patient infected with Puumala virus (Terajima et al., 2002). 1A-E2 was maintained in RPMI (Invitrogen Corporation) containing 10% FCS.

2.2. HLA-typing of EA.hy926 cells

HLA-type of EA.hy926 cell line was determined by RT-PCR and nucleotide sequencing as described previously (Co et al., 2002). Total RNA was extracted from EA.hy926 cells. cDNA was synthesized. HLA-A, B and C genes were amplified using common 5′ primer, HLA-5P2 containing *Sal*I restriction enzyme site, and HLA-A, B and C-specific 3′ primers, HLA-3PA, HLA-3PB, and HLA-3PC containing *Hind*III restriction enzyme site, respectively (Zemmour et al., 1992). These PCR products were cloned into the pBluescript II SK(+) vector. Six plasmid clones from each of the HLA alleles were purified, and the nucleotide sequences were determined. The PCR products were also directly sequenced (Ennis et al., 1990). The sequencing reactions were performed by the Nucleic Acid Facility of the University of Massachusetts Medical School. These sequencing results showed that the EA.hy926 cell line expressed HLA-A*2402, A*2501, B*1501, B*1801, Cw*0303, and Cw*1203.

2.3. Virus titration

Titers of SNV were determined in a focus-forming assay with some modifications (Takashima et al., 1997). Briefly, confluent Vero E6 cells in 96-well plates were inoculated with serially

diluted culture supernatants in 2% FCS DMEM. After 90 min of incubation, virus inocula were removed and cells were washed with PBS. Infected cells were incubated in 2% FCS DMEM containing 1.5% carboxymethylcellulose (Sigma, St. Louis, MO) for 7 days. Virus foci were detected using a rabbit anti-SNV serum (kindly provided by Patrick C. Stockton and Thomas G. Ksiazek) (Zaki et al., 1995) and using a peroxidase-anti-peroxidase (PAP) staining technique (Polysciences, Warrington, PA) combined with DAB Substrate Kit for peroxidase (Vector Laboratories, Burlingame, CA). Foci were counted under a dissecting microscope. Virus titers were calculated as average number of foci in triplicate wells.

2.4. Virus growth curve and Western blotting

Confluent Vero E6 cells and EA.hy926 cells were infected with SNV at multiplicity of infection (m.o.i) of 0.0025 in 6-well plates.. At 0, 1, 4, 8 and 12 days post-infection, supernatants and cells were harvested separately, and stored at −80 °C until use. Virus titers in supernatants were determined by the focus-forming assay described above. Cell lysates were separated in a 10% sodium dodecyl sulfate-polyacrylamide gel electrophoresis (SDS-PAGE) and transferred onto PVDF membranes as previously described (Maeda et al., 2005). SNV proteins were detected by rabbit anti-SNV serum (Zaki et al., 1995) and visualized by Opti-4CN Detection kit (Bio-Rad Laboratories, Hercules, CA).

2.5. Trypan blue exclusion test

Confluent Vero E6 cells and EA.hy926 cells in 96-well plates were infected with SNV at an m.o.i of 0.01 or 0.001 in triplicates. At 1, 3, 6 and 9 days post-infection, both adherent and detached cells were harvested, and resuspended in 0.2% Trypan blue solution. Stained and unstained cells were counted under microscopy.

2.6. Measurement of lactate dehydrogenase (LDH) activity in the supernatants of SNV infected cells

Confluent Vero E6 cells and EA.hy926 cells in 96-well plates were infected with SNV or recombinant adenovirus containing the cDNA encoding the SNV G2 protein. At 3, 6 and 9 days post-infection, supernatants were collected and LDH activity released from the cytosol of damaged cells into the culture supernatant was measured in triplicates by Cytotoxicity Detection Kit (LDH) (Roche Applied Science, Mannheim, Germany) following the manufacturer's protocol. Relative LDH activity in the supernatants was calculated as follows.

$$\text{relative LDH activity (\%)} = \frac{\text{experimental value} - \text{low control}}{\text{high control} - \text{low control}} \times 100$$

High control in the assay was uninfected cells treated with 2% Triton X-100 solution for 10 min. Low control was uninfected cells incubated with culture medium alone.

2.7. CTL assay

Confluent EA.hy926 cells were infected with SNV at m.o.i of 0.01 in 96-well flat-bottom plates. At 3 days post-infection, medium was removed and cells were washed with PBS, then 1A-E2 cells were added as effector/target (*E/T*) ratio of 1 and incubated for 4 or 16 h. Supernatants were harvested and CTL activity was measured by Cytotoxicity Detection Kit (LDH) (Roche Applied Science) described in the previous subsection (2.6). In the CTL assays low control was infected cells incubated without effector cells (1A-E2). 10% specific lysis above background was considered positive.

2.8. Transwell permeability assay

The assay was performed following the previously published method with some modification (Shaw et al., 2001). EA.hy926 cells were cultured in 24-well transwell inserts (Polycarbonate membrane Transwell® Inserts, Corning Incorporated, Acton, MA). Confluent EA.hy926 cell monolayers were infected with SNV at m.o.i. of 0.01 in the upper chambers. After 90 min of incubation, virus inocula were removed and washed with PBS. Infected monolayers were incubated in 2% FCS DMEM. Three days after infection, 1A-E2 cells were added at *E/T* ratio of 1 (for wells without CTL, only media were changed), and cells were incubated for 16 h. Then, media in the upper chambers were replaced with fresh media containing 500 μg/ml of f-dextran (dextran, fluorescein, 70,000 MW, anionic, Molecular Probes, Eugene, OR). The media in the lower wells were taken at 0, 15 and 30 min and the absorbances at 485 nm wavelength were measured. Since we observed an increase in the permeability in negative control wells ("media" in Fig. 5) after 30 min of incubation in the first set of the assays, we used earlier time points (0, 10 and 20 min) in the next set of the assays. The concentrations of f-dextran were calculated from a standard curve.

2.9. Generation of recombinant adenoviruses expressing the SNV G2 protein

A recombinant adenovirus which expresses the SNV G2 protein was constructed as we reported previously (Maeda et al., 2005). An Adenovirus Expression Vector Kit (Takara Shuzo, Kyoto, Japan) was used. The full-length SNV G2 protein cDNA was excised from the plasmid, pGEM-G2 (kind gift from Christina Spiropoulou of the CDC), with restriction enzyme *BamH*I and *Eco*RI, blunt-ended with Klenow fragment, and inserted into the cosmid vector, pAxCAwt, at its *Swa*I site. The cosmid carrying the SNV G2 cDNA under the control of the strong CAG promoter, pAxCAwt-SNV-N, was packaged using GigapackR III XL packaging extract (Stratagene, La Jolla, CA). 293 cells (ATCC number CRL-1573) were transfected with pAxCAwt-SNV-G2 and restriction enzyme-digested DNA-TPC using Calcium Phosphate Transfection Kit (Invitrogen). Recombinant adenovirus, rAd-SNV-G2, was cloned by limiting dilution and grown in 293 cells for preparation of high-titer virus stock solutions. Viral titers were determined by the 50% tissue culture infectious dose ($TCID_{50}$) method in 293 cells.